

8-2011

Sensitivity Analysis of Load Distribution in Light-Framed Wood Roof System due to Typical Modeling Parameters

Ranjith Shivarudrappa
Clemson University, rnths10@gmail.com

Follow this and additional works at: https://tigerprints.clemson.edu/all_theses

 Part of the [Civil Engineering Commons](#)

Recommended Citation

Shivarudrappa, Ranjith, "Sensitivity Analysis of Load Distribution in Light-Framed Wood Roof System due to Typical Modeling Parameters" (2011). *All Theses*. 1174.

https://tigerprints.clemson.edu/all_theses/1174

This Thesis is brought to you for free and open access by the Theses at TigerPrints. It has been accepted for inclusion in All Theses by an authorized administrator of TigerPrints. For more information, please contact kokeefe@clemson.edu.

SENSITIVITY OF LOAD DISTRIBUTION IN LIGHT-FRAMED WOOD ROOF
SYSTEMS DUE TO TYPICAL MODELING PARAMETERS

A Thesis
Presented to
the Graduate School of
Clemson University

In Partial Fulfillment
of the Requirements for the Degree
Master of Science
Civil Engineering

by
Ranjith Shivarudrappa
August 2011

Accepted by:
Dr. Bryant G. Nielson, Committee Chair
Dr. Scott D. Schiff
Dr. Weichi Pang

ABSTRACT

Since failure of roof systems in past high wind events have demonstrated the consequences of not maintaining a continuous load path from the roof to the foundation, many studies have been conducted to better understand this load path, including how loads are distributed in the system. The present study looks to add to the current knowledge of the vertical load path by focusing on uplift loads and by considering the sensitivity of different modeling parameters. This is done by developing and assessing load influence coefficients for various roof-to-wall (RTW) connections. An analytical model of a light-framed wood structure using finite element software is developed. The model has a gable roof system comprised of fink trusses and is modeled in a highly detailed fashion including the explicit modeling of each connector/nail in the system.

The influence coefficient plots indicate that the distribution of loads is indeed sensitive to the overall stiffness of RTW connections but is not overly sensitive to their relative stiffnesses. This was investigated by looking at cases where all connections have the same stiffness and cases where they can have different stiffnesses. However, the relative stiffness begins to have a larger impact as they begin to soften due to yielding. Furthermore, the stiffness of the sheathing connectors did not appear to have much of an impact on the distribution of load but the sheathing stiffness itself did have a notable impact.

ACKNOWLEDGEMENTS

I would like to express my sincere appreciation for the guidance and support my committee chair, Dr. Bryant G. Nielson, has provided to me throughout my work on this document. This work was accomplished with his mentoring, enthusiasm, knowledge and consistently positive attitude which also kept me going throughout my graduate work. I would also like to thank my committee members – Dr. Scott D. Schiff and Dr. Weichiang Pang – for their help and support during various aspects of my research and graduate studies.

Additionally, I would like to acknowledge Dr. Bagyalakshmi Shanmugam for developing analytical model which helped me to begin my work and Dr. Peter Leroy Datin for his paper, “Experimentally Determined Structural Load Paths in a 1/3-Scale Model of Light-Framed Wood, Rectangular Building” which served as basis for my study.

Finally, I wish to thank my parents for their encouragement and support both emotionally and financially in pursuing an advanced degree.

TABLE OF CONTENTS

	Page
TITLE PAGE	i
ABSTRACT	ii
ACKNOWLEDGEMENTS	iii
LIST OF TABLES	vi
LIST OF FIGURES	vii
CHAPTER	
1. INTRODUCTION.....	1
Outline of Thesis	2
2. LITERATURE REVIEW	4
3. ANALYTICAL MODELING OF ROOF SYSTEM	9
Analytical Model	9
4. LOAD DISTRIBUTION SENSITIVITY STUDY	19
Influence Coefficient Contour Plots	19

Table of Contents (Continued)

	Page
Sensitivity Study.....	20
Linear Behavior Results	24
Nonlinear Behavior Results.....	36
5. CONCLUSIONS.....	43
REFERENCES	46
APPENDIX	
A. INFLUENCE COEFFICIENT CONTOURS	49

LIST OF TABLES

Table	Page
3.1 Roof-to-wall connector (2-16d toe-nails) uplift model parameter statistics	16
3.2 Sheathing connector (8d-box nails) withdrawal parameters.....	17
4.1 Outline of scenarios used for sensitivity study	23

LIST OF FIGURES

Figure		Page
2.1	Vertical structural load paths	5
3. 1	Typical roof truss configuration.....	10
3. 2	Details of gable end truss	11
3. 3	Layout of sheathing panels and sheathing connectors	13
3. 4	Connection schematic	14
3. 5	Backbone curve for toe-nail uplift behavior	16
3. 6	Backbone curve for sheathing connector uplift behavior	18
4. 1	Influence line (coefficient) sample calculation.....	19
4. 2	Influence coefficient contours for setup 1 (median values) a) RTW No. 6 b) RTW No. 7	25
4. 3	Influence coefficient contours for setup 8 (gravity) a) RTW No. 6 b) RTW No. 7	26
4. 4	Normalized reactions of RTW connectors when the load is applied distances a) 0 mm (in) b) 610 mm (24 in) c) 1220 mm (48 in) and d) 1831 mm (72 in) from RTW No. 6.....	28
4. 5	Normalized reactions of RTW connectors when the load is applied distances a) 0 mm (in) b) 610 mm (24 in) c) 1220 mm (48 in) and d) 1831 mm (72 in) from RTW No. 7.....	29
4. 6	Influence coefficient contours for setup 2 (low RTW stiffness) a) RTW No. 6 b) RTW No. 7.....	30

List of Figures (Continued)

Figure	Page
4. 7	Influence coefficient contours for setup 3 (high RTW stiffness) a) RTW No. 6 b) RTW No. 7 30
4. 8	Influence coefficient contours for setup 4 (Random RTW connector stiffness) a) RTW No. 6 b) RTW No. 7 31
4. 9	Influence coefficient contours for setup 5 (Random sheathing connector stiffness) a) RTW No. 6 b) RTW No. 7..... 32
4. 10	Influence coefficient contours for setup 6 (low sheathing stiffness) a) RTW No. 6 b) RTW No. 7..... 33
4. 11	Influence coefficient contours for setup 7 (high sheathing stiffness) a) RTW No. 6 b) RTW No. 7..... 33
4. 12	Influence coefficient contours for RTW No. 1 for a) setup 1 (median values) b) setup 9 (no gable connections) 34
4. 13	Influence coefficient contours for RTW No. 7 for a) setup 1 (median values) b) setup 9 (no gable connections) 35
4. 14	Influence coefficient contours for setup 10 (rafter framing) a) RTW No. 6 b) RTW No. 7 36
4. 15	Influence coefficient contours for setup 11 (slight nonlinearity) a) RTW No. 6 b) RTW No. 7 37
4. 16	Influence coefficient contours for setup 12 (moderate nonlinearity) a) RTW No. 6 b) RTW No. 7 38
4. 17	Force displacement behavior of RTW connector no.7 when the load is applied distances a) 0 mm (0 in), b) 610 mm (24 in) and c) 1831 mm (72 in) from RTW No. 7..... 39

List of Figures (Continued)

Figure	Page
4. 18 Force displacement behavior of sheathing connectors at distances 0 mm (0 in), b) 610 mm (24 in) and c) 1831 mm (72 in) from RTW No. 7 when load placed over respective connectors.....	41
A. 1 Influence coefficient scale	49
A. 2 Influence coefficient contours for setup 1.....	52
A. 3 Influence coefficient contours for setup 1(contd.).....	53
A. 4 Influence coefficient contours for setup 2.....	54
A. 5 Influence coefficient contours for setup 2(contd.).....	55
A. 6 Influence coefficient contour for setup 3	56
A. 7 Influence coefficient contour for setup 3(contd.).....	57
A. 8 Influence coefficient contour for setup 4	58
A. 9 Influence coefficient contour for setup 4(contd.).....	59
A. 10 Influence coefficient contour for setup 5	60
A. 11 Influence coefficient contour for setup 5(contd.).....	61
A. 12 Influence coefficient contour for setup 6	62
A. 13 Influence coefficient contour for setup 6(contd.).....	63
A. 14 Influence coefficient contour for setup 7	64
A. 15 Influence coefficient contour for setup 7(contd.).....	65
A. 16 Influence coefficient contour for setup 8	66
A. 17 Influence coefficient contour for setup 8(contd.).....	67

List of Figures (Continued)

Figure		Page
A. 18	Influence coefficient contour for setup 9	68
A. 19	Influence coefficient contour for setup 9(contd.).....	69
A. 20	Influence coefficient contour for setup 10	70
A. 21	Influence coefficient contour for setup 10(contd.).....	71
A. 22	Influence coefficient contour for setup 11	72
A. 23	Influence coefficient contour for setup 11(contd.).....	73
A. 24	Influence coefficient contour for setup 12	74
A. 25	Influence coefficient contour for setup 12(contd.).....	75

CHAPTER ONE

INTRODUCTION

During the lifetime of a structure, it will be subjected to various structural loads which it must be able to handle. To perform at an acceptable level, the structure must be able to take these applied loads and safely transfer them to the foundations; otherwise failure – unwanted performance – will occur. In addition to having sufficient strength in the members it is essential that an adequate load path is established in the structure since it governs the overall stability during both service level and extreme level loading events. Therefore any structure needs to be assessed with careful understanding and evaluation of load paths in order to avoid significant damage (Taly 2003). For example, in wind storms, the wind uplift forces must be transferred from the roof and walls to the foundations through a complete and continuous load path. Loss of load carrying capacity in any of the elements within the load path will result in an explicit discontinuity which can destroy structural stability. In low-rise light-frame wood roof structures, roof-to-wall(RTW) connections and sheathing connections are critical yet traditionally vulnerable elements in the vertical load path during extreme wind events such as hurricanes. If any of these components fail either local or global structural instabilities can occur.

Hurricanes can cause major economic losses in the form of failures in residential wood-framed construction. Failure of RTW connections and loss of roof sheathing panels during high wind events is one of the most common types of recorded failure (Bhaskaran

et al 1997). Wood structures can undergo slight structural damage while remaining intact during extreme winds but extreme damage occurs when the roof system is damaged partially or completely due to the improper vertical load paths. (Reed et al 1997; van de Lindt et al 2007). Add this to the fact that according to the U.S. Census Bureau (2010), more than half of the country's population lives in the coastal counties (including the West coast) – an area highly prone to hurricanes and one may quickly realize the significance of ensuring adequate performance of residential structures.

The specific objectives of this study are:

- To determine the load distribution (influence coefficient contours) due to both uplift and gravity loads.
- To understand the sensitivity of load distribution due to changes in different modeling parameters like sheathing panel stiffness, connector stiffness, type of framing and loading.
- To determine the effect of gable truss connections.
- To verify the load distribution when the applied load causes connectors to behave in a nonlinear fashion.

Outline of Thesis

The remaining Chapters of this thesis include discussion on previous studies, modeling procedures, analysis, load distribution and conclusions drawn. A brief but relevant literature review is presented in Chapter 2 while Chapter 3 focuses on the

development of the computer model utilized in the analysis. Chapter 4 provides a discussion on the load distribution, sensitivity study and influence coefficients with linear and nonlinear behavior results. Conclusions drawn from this study are discussed in Chapter 5.

CHAPTER TWO

LITERATURE REVIEW

When any form of load is applied on a structure, it follows its own path to reach the foundation from the point of load application. As shown in Figure 2.1 a continuous vertical load path to resist wind uplift forces exists in typical wood roof structures. Wind loads which act normal to roof coverings are transferred to roof sheathing panels which then send the loads through sheathing connectors to the roof trusses or rafters. The roof trusses transfer the forces into the walls through a connection made at their interface, commonly referred to as a roof-to-wall (RTW) connection. The load then continues through the walls and into the foundation via anchor bolts and hold-downs or straps. Each of the members and connections in this load path must be adequate to resist these uplift loads, the failure of which could compromise the integrity of the entire structure by breaking up the requisite load path. Thus, both the connections and members must be designed appropriately to transfer the applied loads, which imply that a good understanding of the applied loads must first be obtained.

Having a limited knowledge regarding the actual load paths within a three-dimensional (3D) wood framing system, modeled with the multiple load paths, can contribute to poor performance of these structure types during extreme wind events. Obtaining this understanding can further be complicated by the fact that these structures have elements which can behave nonlinearly (metal plate trusses, nails in withdrawal, etc.) and cause a redistribution of forces within the system.

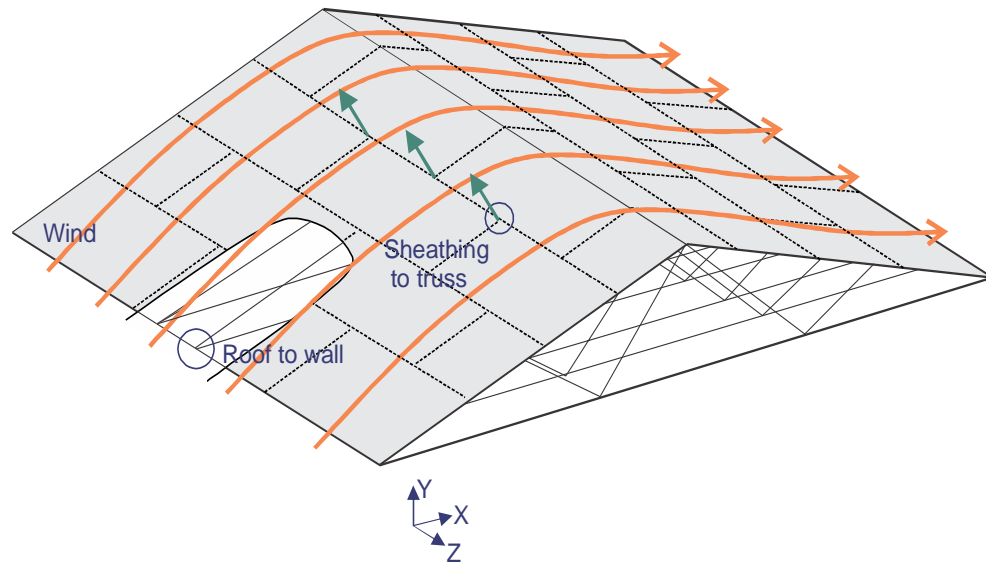


Figure 2. 1: Vertical structural load paths (adapted from Shanmugam et al. 2008)

Understanding the structural load paths and load transfer mechanisms in light frame wood roof (LFWR) systems is significant to improving the prediction of structural failures in extreme wind events. Furthermore, the need for knowledge on the system behavior of complex roof truss assemblies in transmission and distribution of loads is significant for economic and safe design of trusses (Gupta 2005).

To help in identifying the actual loads which exist in a light-frame wood roof assembly Cramer et al.(1989) performed a study on its load distribution characteristics. This was done by creating an analytical model exclusively using line elements, then by applying loads and observing the way they distribute through the system. Relative flexural stiffness of sheathing elements and truss members clearly affected the way gravity loads are distributed in the system. Indeed, when the top chord of an individual truss was loaded to the design load, the loaded truss in the assembly carried only 40-70

percent of the applied load and distributed the remaining load to the adjacent unloaded trusses through the plywood sheathing. (Wolfe et al. 1991)

One way of understanding how loads distribute through a roof system is to develop load influence coefficient functions for the RTW connections. These functions have been previously explored for low-rise wood structures for uplift loads (Mani 1997). The influence extended as far as one truss on either side for the interior connections. Furthermore, the intermediate connections along gable end trusses caused the influence to taper off from the eaves (Datin 2010).

Identifying load paths in light frame wood buildings subjected to environmental loads has been achieved by conducting experiments at the element level, subsystem level and on the whole building level with prediction of interaction between the roof system and the walls. The responses of these buildings to controlled static tests as well as natural environmental loads were observed and compared with a wind tunnel study and with detailed finite element models with good agreement (Doudak 2005). When combined with analytical models these experimental studies can (Datin 2010; LaFave et al. 1992) also refine the prediction the distribution of loads in wood truss roof systems. It is noteworthy to mention that these studies did focus on the linear elastic response of the structure which is not necessarily always the case during extreme wind events. Furthermore, the effect of the connectors, sheathing panels and their interaction as a whole system has often been overlooked in the past. Connector stiffness, for instance the nail stiffness, has little effect on load sharing and load redistribution without affecting the system reserve capacity significantly. (Liu et al. 1995)

When an analytical model is created using a structural analysis program, the designer has to decide the method of connecting the structural members to one another. Truss joints can be considered either as pinned (Martin 2010) or as semi-rigid (Li et al 1998). Linear spring elements representing semi-rigid behavior at truss joints can be used in the computer program (Li et al 1998; Cramer et al 2000).

Load sharing is one of the main structural benefits of sheathing. It facilitates the redistribution of forces among individual members within an assembly. Members that are not identical, with varying connections cause differential deflections resulting from installation (i.e. uneven surfaces). Sheathing assists in distributing load away from flexible members towards those which are more stiff (Li et al. 1998). As a result, the goal of any analytical model is to address these effects when incorporating sheathing products into the model. Though the sheathing elements modeled as continuous beam elements on the top chord (Cramer et al. 2000) or beam elements with pin joints representing the discontinuity in sheathing (Li et al 1998) are in good agreement with experimental results, the effect of sheathing fasteners is not captured.

The present study looks to add to the current understanding in load distribution in wood frame roof systems subjected to uplift loads. Through the use of a three dimensional finite element model the effects of the connector behavior and other modeling parameters on the overall behavior of the complex roof system is evaluated. The RTW connectors and sheathing connectors, which are considered in both the linear

and nonlinear range, are treated in a sensitivity study to identify their significance to system behavior.

CHAPTER THREE

ANALYTICAL MODELING OF ROOF SYSTEM

Analytical Model

The roof structure selected for this study is modeled after the experimentally tested structure developed by Datin et al. (2008) and is adapted from the model originally created by Shanmugam (2011). The 3-D model of the roof system was modeled using the commercially available general finite element package ANSYS (2009). In order to create the model with number of elements not exceeding the allowable limits of the package, half of the structure is modeled. The selected roof consists of 13 fink trusses spaced at 0.6 m (24 in.) on center as shown in Figure 3.1. Each truss has a span of 9.1 m (360 in.) and a ridge height of 1.5 m (60 in.) resulting from a pitch of 4 in 12 (Datin et al. 2008). Each of the fink trusses has four web members connecting the top chord to the bottom chord. One of the trusses at the end is a gable end truss which consists of vertical web members spaced at 0.6 m (24 in.) on center as seen in the Figure 3.2. The joint between the web members and the chord members are considered to be pinned in all cases. This configuration was also used successfully in the research effort conducted by Gupta et al (2008). RTW connectors investigated in the study are selected from the center of the roof truss and hence the nodes along the symmetrical line i.e. truss 13 are not restrained in rotation.

Both the truss chords and web members have dimensions of 38.1 mm (1.5 in.) by 88.9 mm (3.5 in.) in cross section. The top chords are connected to the top plate of the

wall through RTW connectors. The truss members are modeled using the BEAM4 element; a frame element with tension, compression, torsion, and bending capabilities. Elastic shell elements (SHELL63) are used to model the sheathing panels. Furthermore, with bending and membrane capabilities, both in-plane and out-of-plane action can be captured.

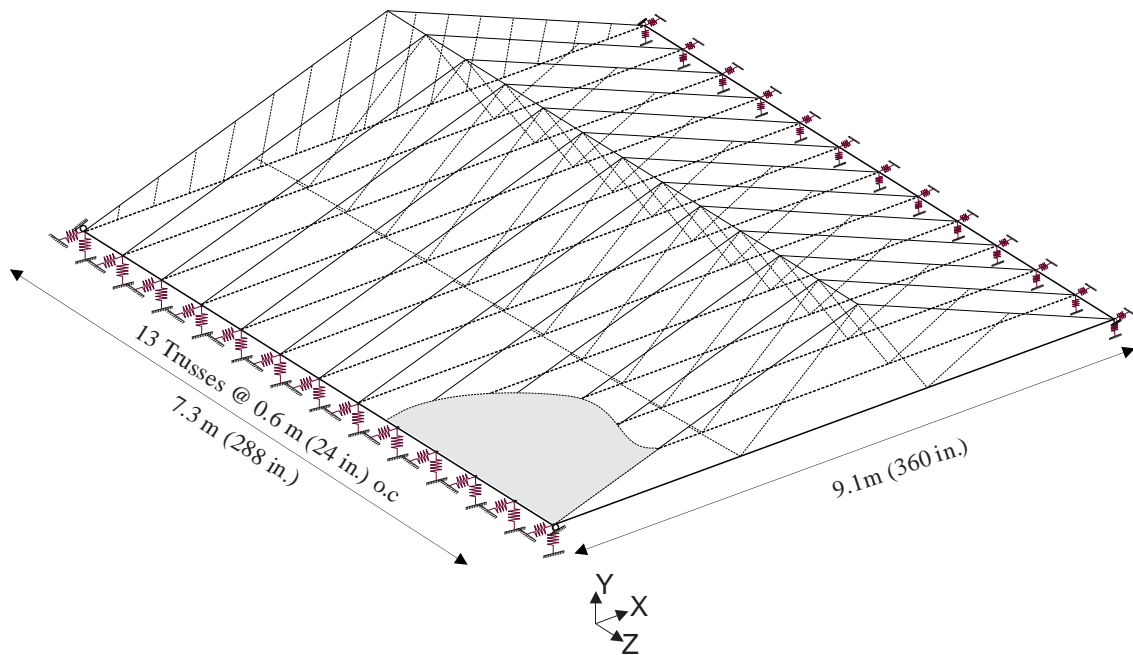


Figure 3. 1: Typical roof truss configuration

The trusses are assumed to be constructed out of Southern Yellow Pine (SYP). The modulus of elasticity is taken as 11.72 GPa (1700 ksi) (Wolfe et al. 1991) and the Poisson's ratio is taken as 0.40 (Martin 2010). Both the upper and the lower chords are modeled as continuous members and are only pinned at the ridge and at the heels. The

web members are then pin connected to the chords. Though there are joints along the bottom chord, it is assumed to be continuous as the effect of them on the stiffness of RTW connectors is very minor.

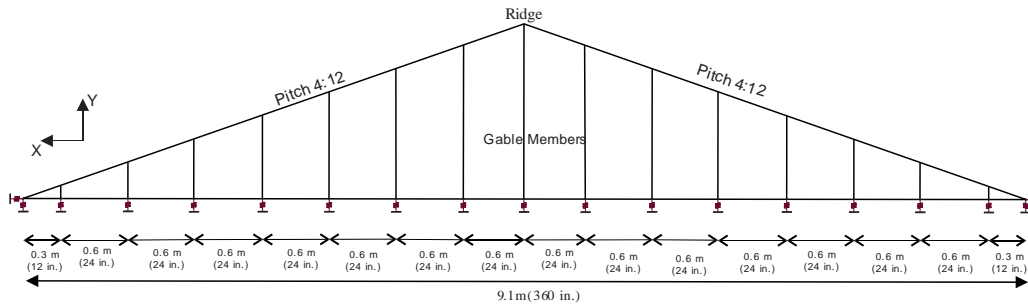


Figure 3. 2: Details of gable end truss

The structural roof sheathing was oriented with its strong axis parallel to the ridgeline of the roof. The panel joints are staggered as shown in Figure 3.3 to capture the realistic behavior resulting from having discontinuous panels across the entire roof. Roof panels had dimensions averaging 2438 mm (96 in.) long by 1219 mm (48 in.) wide with a thickness of 11.9 mm (15/32 in.). Each panel is connected to the top truss chord using sheathing connectors spaced at 152.5 mm (6 in.) from center to center along the edges of the panel and at 304.8 mm (12 in.) on center along the intermediate supports (“the field”) of the panel. The sheathing connectors of all panels are assumed to connect at the centerline of the truss. They are considered to provide resistance in only the translational degrees of freedom and thus are modeled as 3-axis nonlinear translational springs – the behavior of which will be described later in this manuscript (see Figure 3.4).

To more fully facilitate the evaluation of roof system responses, including the distribution of load, this analytical model uses nonlinear models for both the RTW toenail connectors and the sheathing connectors instead of the traditionally used pin connections (Martin 2010). The connectors are characterized by three main behaviors; uplift nail withdrawal and the two orthogonal shears. The analytical model presented herein is designed to capture these three behaviors but specific focus is given to capturing the behavior under uplift nail withdrawal since this is the primary load which is applied in a wind event for low angle roofs. In the past, these connections have generally been modeled as pinned connections having a specified uplift capacity. This specific assumption fails to simulate the actual nonlinear response and subsequent failure of such connections – including post-ultimate behavior – when exposed to high loads (Shanmugam 2011).

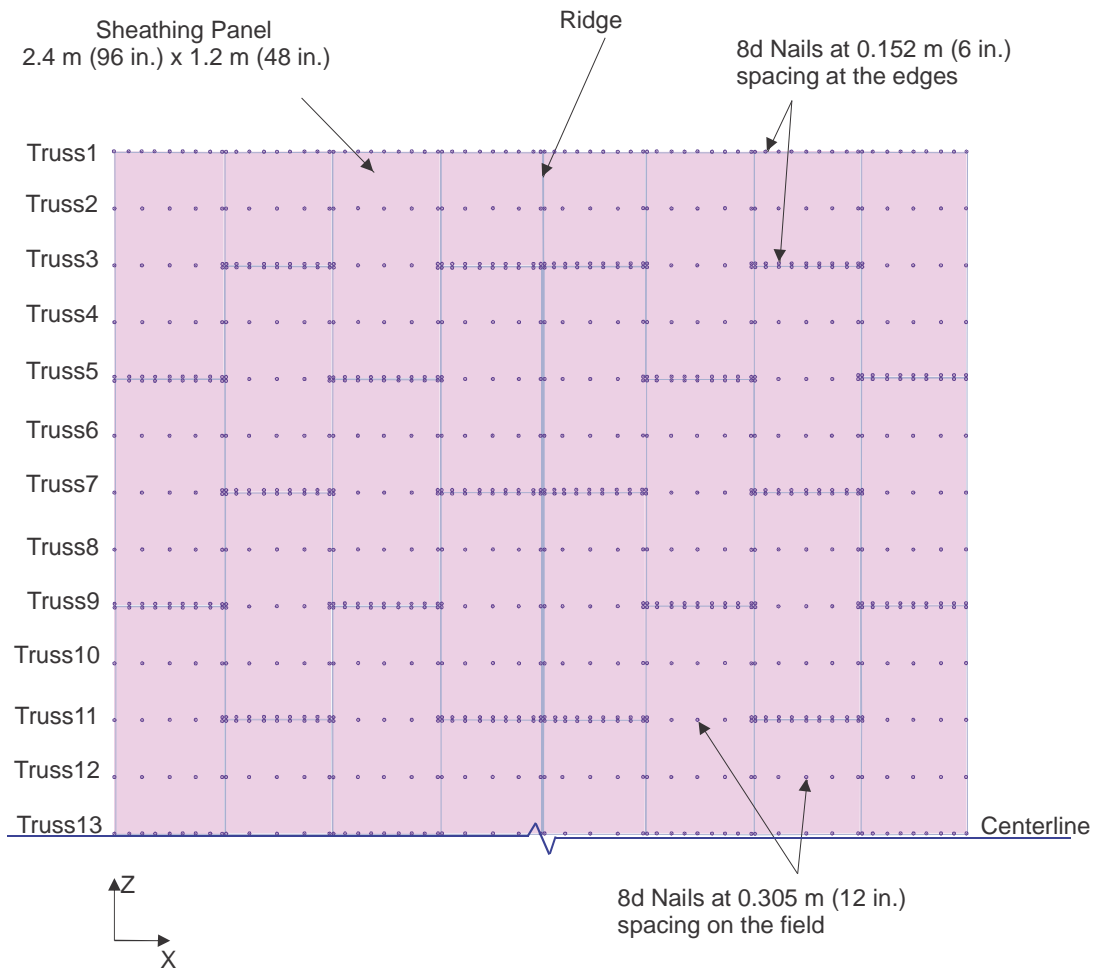


Figure 3. 3: Layout of sheathing panels and sheathing connectors

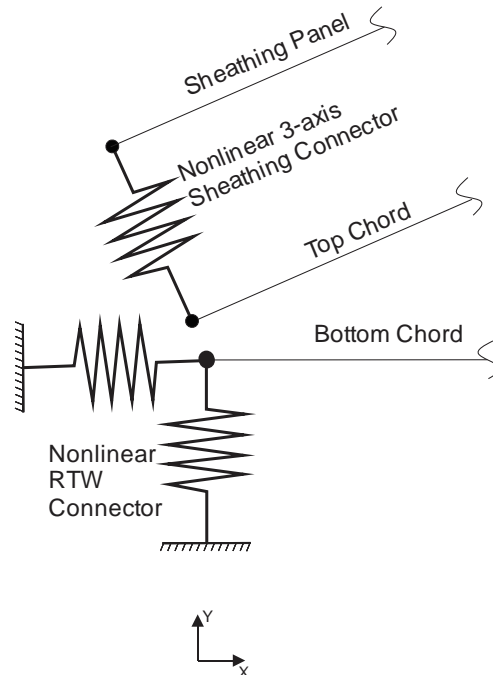


Figure 3. 4 Connection schematic

The RTW connection is modeled using the COMBIN39 ANSYS element (Silva et al. 2005); a unidirectional element with nonlinear generalized force-deflection capability that can be used in the analysis. A model for toe-nailed RTW connections, which has been proposed by Shanmugam et al. (2009), is used in this study. It requires three main parameters to define the backbone curve which are the ultimate uplift capacity (F_{ult}), initial secant stiffness (k_o) and displacement at peak load (δ_{PL}) which are shown on Figure 3.5. The yield force of the toe-nail is defined as two thirds of the ultimate uplift force. The maximum displacement at which all strength is lost is taken to be 66 mm (2.63 in.) which is an approximate displacement value for complete withdrawal of the toe-nails. In

addition to connection model behavior, Shanmugam et al. (2009) also provided appropriate probability models for describing these three parameters - $F_{ult} \sim LN$, $k_o \sim N$ and $\delta_{PL} \sim W$. There exists complete correlation between the parameters. The correlation coefficients between the ultimate uplift capacity and initial secant stiffness, $(\rho F_{ult}, k_o)$ is 0.62, the ultimate uplift capacity and displacement at peak load, $(\rho F_{ult}, \delta_{PL})$ is 0.393 and the initial secant stiffness and displacement at peak load, $(\rho k_o, \delta_{PL})$ is 0.096. These coefficients are used to obtain the RTW connector parameters for random stiffness case through a set of non-normal correlated probability distribution using Nataf transformation in accordance with Appendix B of reliability text (Melchers 2001). For this study, certain percentiles for these model parameters are considered and are presented in Table 3.1. The 5th percentile value is considered to represent the case with low RTW connector stiffness. When the model is generated all 26 RTW connectors are assigned this value. The 95th percentile values are considered for the case with high RTW connector stiffness. For the other cases, the RTW connectors are assigned the median values.

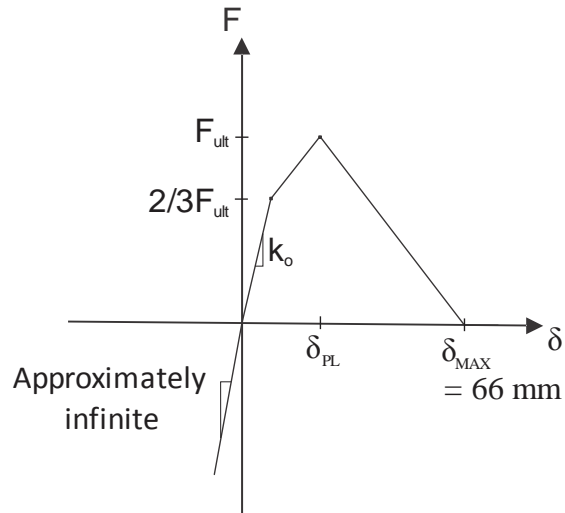


Figure 3. 5: Backbone curve for toe-nail uplift behavior

Table 3. 1: Roof-to-wall connector (2-16d toe-nails) uplift model parameter statistics

Level	Uplift Capacity (F_{ult}) kN (lbs)	Initial Stiffness (k_0) kN/mm (lbs/in)	Displacement at Peak Load (δ_{PL}) mm (in)
Low (5 th percentile)	2.55 (574.6)	0.15 (868)	23.1 (0.91)
Median	1.44 (323.1)	0.37 (2126)	9.7 (0.38)
High (95 th percentile)	0.81 (181.7)	0.59 (3384)	4.2 (0.16)

The shear properties of the RTW connector elements are considered to be deterministic in this study and are considered to be symmetric having a bi-linear elastic-perfectly plastic behavior with an initial stiffness of 0.98 kN/mm (5600 lb/in) and yield force of 4.23 kN (950 lb). The values for this model are derived from experiments conducted by Edmonson et al. (2011).

Sheathing connectors are modeled using the work by Dao et al. (2008) as 8d box nails with a length of 60 mm (2.4 in.) and a diameter of 3 mm (0.113 in.). The test data were used to develop an appropriate probability distribution model of nail withdrawal capacity. Statistics regarding this nail behavior which are relevant to the current study are given in Table 3.2. When simulation of the nail stiffnesses is needed, the lognormal distribution is assumed with logarithmic standard deviation of 0.185. Sheathing connectors are modeled as elastic materials with parameters such as the ultimate uplift capacity (F_{ult}) and displacement at peak load (δ_{PL}) which are shown on Figure 3.6 to define the backbone curve.

Table 3. 2: Sheathing connector (8d-box nails) withdrawal parameters

Level	Uplift Capacity (F_{ult}) kN (lbs)	Initial Stiffness (k_0) kN/mm (lbs/in)	Displacement at Peak Load (δ_{PL}) mm (in)
Low (5 th percentile)	1.72 (387.0)	0.11 (633)	15.5 (0.61)
Median	1.27 (285.4)	0.44 (2532)	2.9 (0.11)
High (95 th percentile)	0.94 (210.5)	1.77 (10122)	0.5 (0.02)

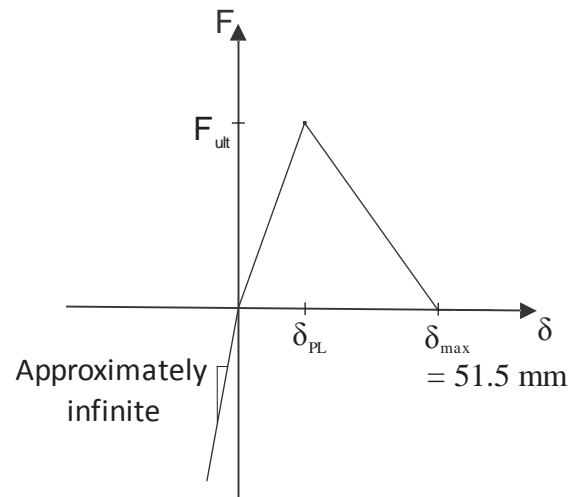


Figure 3. 6: Backbone curve for sheathing connector uplift behavior

The shear behavior of the sheathing connectors is modeled as elastic perfectly plastic in both orthogonal directions. The values of this model are derived from the work by Shirazi et al. (2011) giving a yield strength of 1.18 kN (265 lbs) and a stiffness of 0.178 kN/mm (1020 lb/in).

CHAPTER FOUR

LOAD DISTRIBUTION SENSITIVITY STUDY

Influence Coefficient Contour Plots

The quantitative measure of a specific reaction or internal force, like shear or moment, due to the application of load at a certain point on the structure defines the influence that load has on the specific response of the structure. Graphical representation of an influence coefficient line calculated for a simple beam is depicted in Figure 4.1. The influence coefficient is the ratio of the reaction (R) to the applied load (P) at a certain point on the beam.

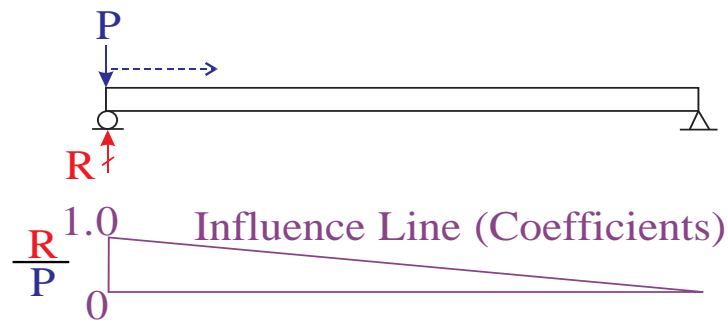


Figure 4. 1: Influence line (coefficient) sample calculation (adapted from Datin 2010)

Following the aforementioned concept, load influence coefficients are developed in this study for various RTW connections in the roof system. These influence coefficients represent the fraction of an applied point load which is experienced in each connector. To create influence coefficient contours the point load, normal to the surface of the sheathing, is applied at a grid spacing of 304.8 mm (12 in.) in both the x and z

directions. Reactions in all 41 RTW connections, which include gable truss connections, are tracked for each loading scenario. The values are then converted to influence coefficients – simply a normalization procedure – and contours are generated to accommodate visual interpretation of the load distribution.

Sensitivity Study

A sensitivity study is the study of the variation in the output of a mathematical model qualitatively or quantitatively, to different sources of variation in the input of the model. It is a method for systematically changing parameters in a model to determine the effects of such changes. In this paper, the study of the load distribution in a LFWR system is performed by analyzing the finite element model with the different setups shown in Table 4.1.

The stiffness of RTW connectors and sheathing connectors, sheathing thickness, type of framing, loading type and the gable member connections to the wall are the main modeling parameters which are investigated in this study. In setup 1, the average stiffness values of both RTW and sheathing connectors are considered. The sheathing thickness is assumed to be 11.9 mm (15/32 in.) which is regarded as the median thickness. The model is generated with interior trusses in fink style with gable end members pin supported on wall. An uplift load of 0.45 kN (100 lbs) is then used to analyze the model.

In setup 2, the lower stiffness value from Table 3.1 is used to define withdrawal behavior of the RTW connectors. Likewise, the higher stiffness value for setup 3 and

random values for all 26 connectors in setup 4 are defined. The remaining inputs remained the same as in setup 1.

The influence of sheathing connector stiffness is investigated in setup 5. This looks at the case where each sheathing connector can have a different initial stiffness as opposed to all having the same stiffness as done in setup 1. The effect of sheathing stiffness is then evaluated in the next two setups where sheathing thickness is changed to 9.5 mm (0.375 in.) in setup 6 and to 15.9 mm (0.625 in.) in setup 7. Although the change in sheathing thickness has an impact on the withdrawal of fasteners, it does not affect the analysis which is linear.

Setup 8 reverses the direction (noted as a gravity case) of the applied load such that all RTW connectors are placed in compression rather than the tension which typically results from uplift loads. The stiffness of RTW connections in compression is very high because the truss bears directly on a wall. However, in tension the stiffness is relatively low because only the toe-nails are providing any resistance. In short, the connection behaves as a pin connection in the gravity case and an elastic support in all other setups.

The impact of the gable end wall connections on load influence is investigated in setup 9 while relative framing stiffness, implemented in the form of different framing schemes, is examined in setup 10. In this setup, the roof system is modeled using rafters which are tied together at their bottom supports with ceiling joist which act as collar ties. Finally, the change in load influence as the connection behavior begins to go nonlinear is

explored in setups 11 and 12 where the applied uplift load is set at 1.78 kN (400 lbs) and 3.56 kN (800 lbs) respectively.

Table 4. 1: Outline of scenarios used for sensitivity study

Setup	Roof to Wall Connectors				Sheathing Connectors		Sheathing Thickness			Framing		Load Application		Gable End		Load Applied, kN (lb)		
	Low	Median	High	Random	Median	Random	Low	Median	High	Truss	Rafter	Uplift	Gravity	Connect to Wall	Not Connect to Wall	0.45(100)	1.78(400)	3.56(800)
1		X			X			X		X		X		X		X		
2	X				X			X		X		X		X		X		
3			X		X			X		X		X		X		X		
4				X	X			X		X		X		X		X		
5		X				X		X		X		X		X		X		
6		X			X		X			X		X		X		X		
7		X			X			X		X		X		X		X		
8		X			X			X		X			X	X		X		
9		X			X			X		X		X			X	X		
10		X			X			X			X		X	X		X		
11		X			X			X		X		X		X			X	
12		X			X			X		X		X		X				X

Linear Behavior Results

Influence coefficient contours make it convenient to understand the load transfer from the point of load application to a given RTW connection. There is a strong similarity in the pattern of the influence coefficient contours for the alternate RTW connections. As such, the influence coefficient contours for only two interior RTW connections are sufficient to facilitate the presentation of findings and discussion throughout this manuscript. These two adjacent connections are selected because of their different proximities to sheathing joints and they are representative of the alternating influence pattern typical to this roof system. As will be discussed later, the presence of sheathing joints in the roof system can have a visible effect on the extent of the load influence. Contour plots for setup 1 are shown in Figure 4.2 which is obtained when a point load of 0.45 kN (100 lb) is applied at multiple locations on the roof individually. One may observe that the peak influence coefficients are centered above or in the proximity of the connector of interest. Around 60 percent of the load applied directly over the connector is transferred to the same connector. The remaining fraction of load is transferred through the sheathing to the adjacent RTW connectors. As the distance of load application increases from the evaluated connector, the connector's share of the load naturally decreases.

The influence coefficient contours show that the load transfer to a given RTW connection typically occurs within one truss space on either side of the connector, a characteristic which has been noted elsewhere (Datin 2010; Mani 1997). However, it is interesting to note the difference in the extent of load influence between RTW No.6 and

RTW No.7 as seen in Figure 4.2. The influence area for connection number 6 is larger than the adjacent connector 7. Close investigation of this phenomenon reveals that this difference is due to the location of sheathing joints which is caused by the staggering of sheathing panels. Whenever a connector is lined up with a sheathing joint in either the first or second row of sheathing, as is the case with connector number 7, the ability of the roof system to transfer load to this connector is limited. However, when the connector does not line up with a sheathing panel joint, as is the case with connector number 6, then the influence area is notably larger. This phenomenon is not able to be detected when a single roof sheathing panel is modeled along the entire length of the roof (Datin 2010; Martin 2010).

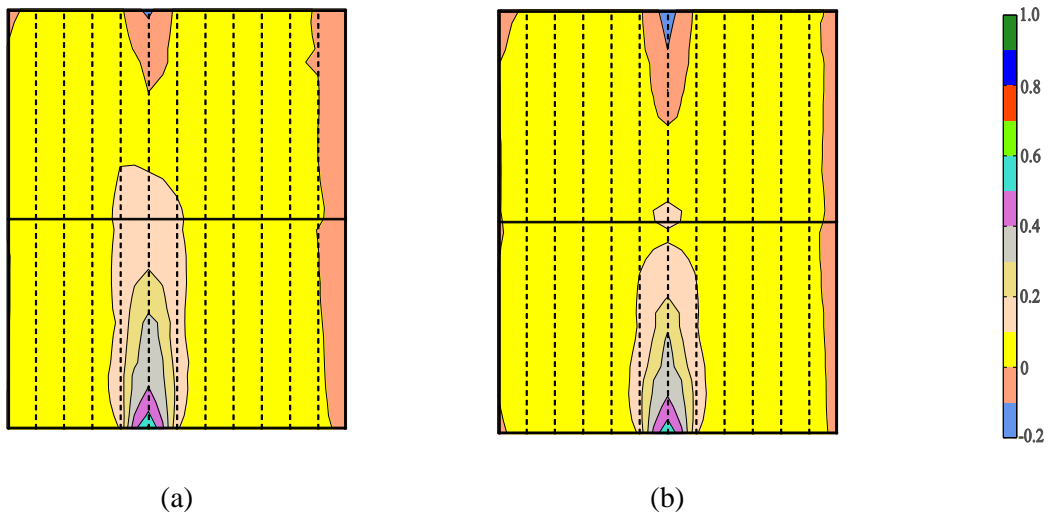


Figure 4. 2: Influence coefficient contours for setup 1 (median values) a) RTW No. 6
b) RTW No. 7

When the RTW connection stiffnesses are increased such that they behave like pin connections instead of elastic connections, as is the case in setup no. 8, the distribution of load changes significantly as shown in Figure 4.3. One may note that when load is placed directly over the connector that around 90 percent of that load is transferred directly down to the connector of interest. This is much different than the 60 percent seen in setup 1 but very close to the over 80 percent which is seen when very rigid connectors are used in an experimental investigation (Datin 2010). Furthermore, the high connector stiffness exacerbates the impact of sheathing joints on the load influence areas as is seen in Figure 4.3.

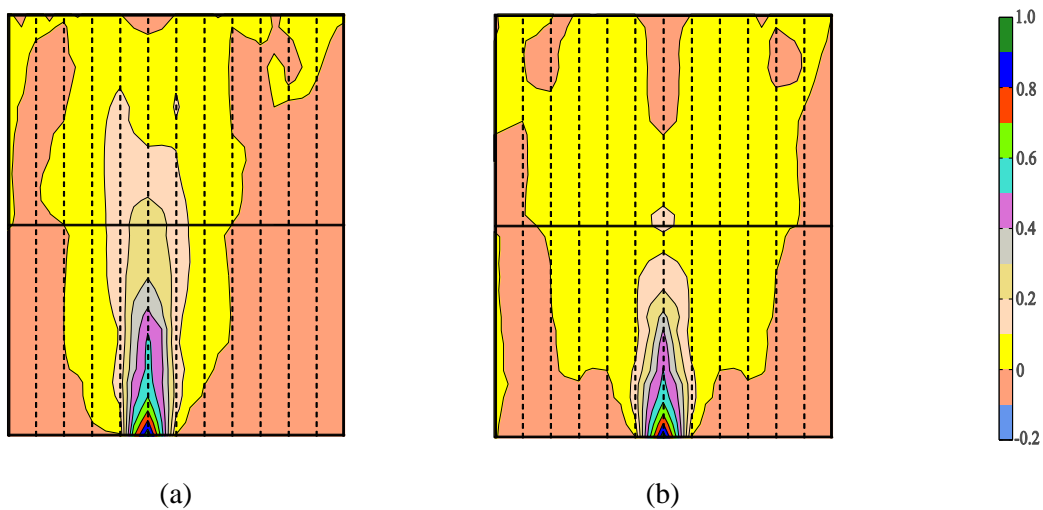
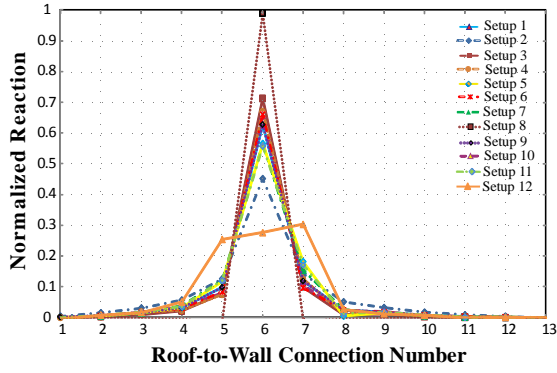


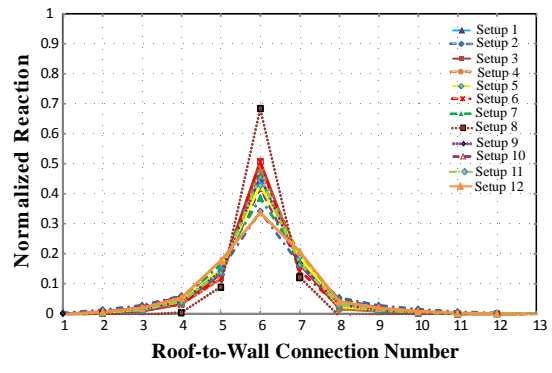
Figure 4. 3: Influence coefficient contours for setup 8 (gravity) a) RTW No. 6
b) RTW No. 7

The plots in Figures 4.4 and 4.5 provide another way of looking at the distribution of load to RTW connectors for a given load location. Four locations of load are considered for comparison including right over the connector, and distances of 610 mm (24 in.), 1220 mm (48 in.) and 1831 mm (72 in.) from the connector. As seen in both figures, the case

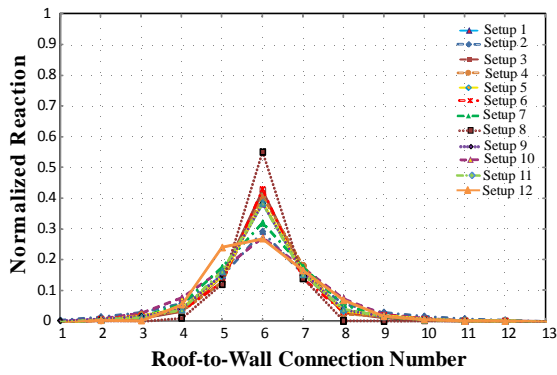
of setup 8 shows the greatest transfer of load to a given connector. However, the attenuation distance from side to side is fairly short evidenced by the fact that for most setups the adjacent connectors take less than 15 percent of the applied load. As the load travels up the truss, as shown in the progression of subfigures a – d, the attenuation distance is greater. When the load is 1831 mm (72 in.) from the connector for that truss, it still takes 50 percent of the load for setup 8 which is the very stiff set of connectors. For the uplift cases, the difference between setups 2 and 3 with different RTW connector stiffness shows differences being in the proximity of 30 percent when the load is applied over the connector and in the range of 12 to 20 percent when it is applied at 1220 mm (48 in.) and 1831 mm (72 in.) away from the RTW connector.



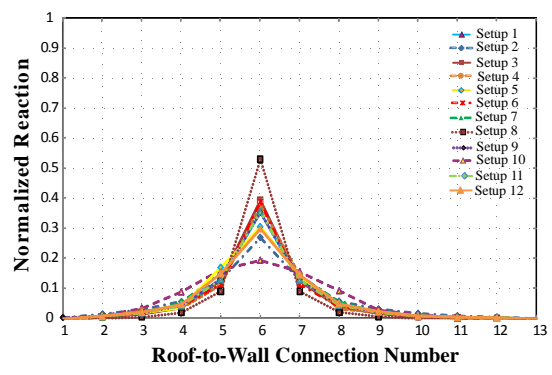
(a)



(b)



(c)



(d)

Figure 4. 4: Normalized reactions of RTW connectors when the load is applied distances
 a) 0 mm (0 in), b) 610 mm (24 in), c) 1220 mm (48 in) and d) 1831 mm
 (72 in) from RTW No. 6

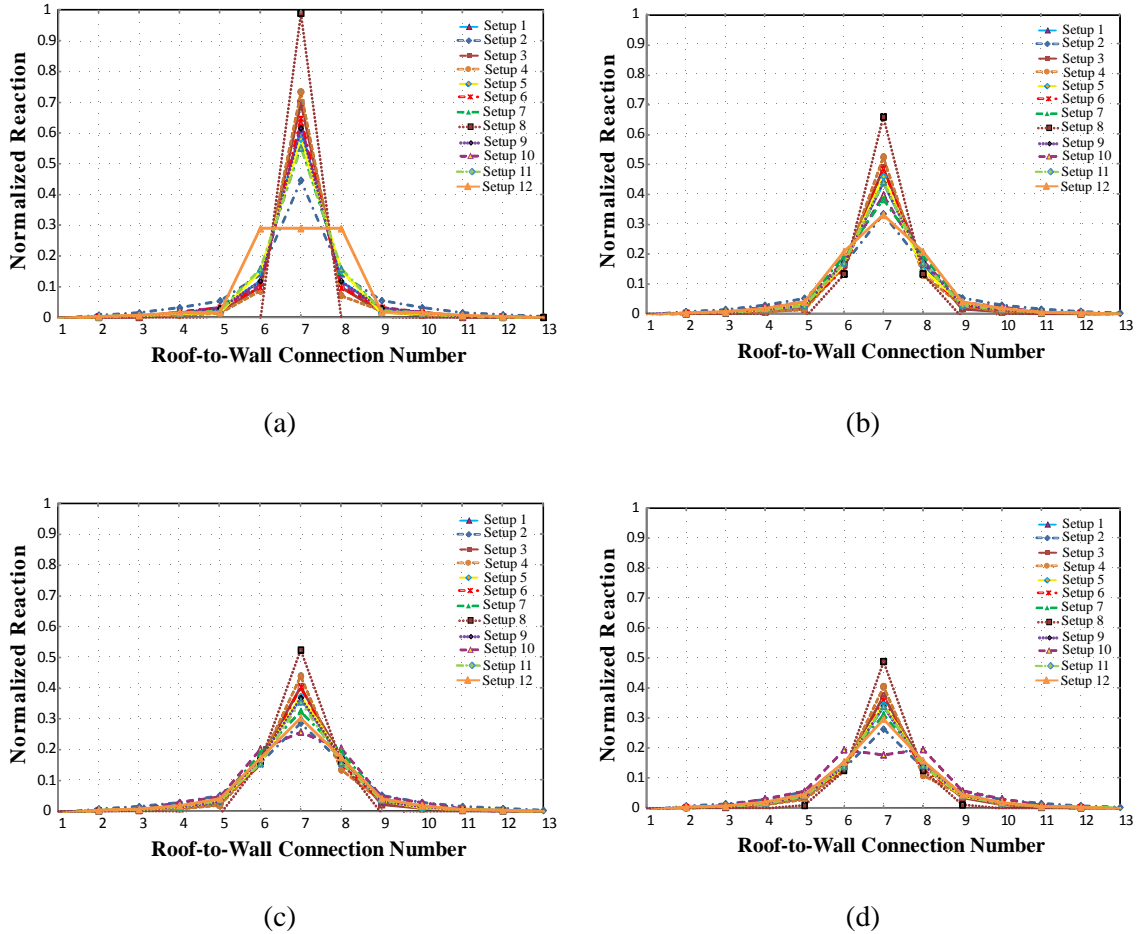


Figure 4. 5: Normalized reactions of RTW connectors when the load is applied distances
a) 0 mm (0 in), b) 610 mm (24 in), c) 1220 mm (48 in) and d) 1831 mm
(72 in) from RTW No. 7

A further look at the impact of RTW connector stiffness is given in Figures 4.6 and 4.7 which use the 5th percentile and 95th percentile connector stiffnesses respectively. In setup 3 the stiffnesses of the RTW connectors are much higher than their counterparts in setup 2. With greater stiffness, the load transferred to the connector is approximately

20 percent higher. However, the width of the influence area remains close to one truss spacing on either side of the connector for both cases.

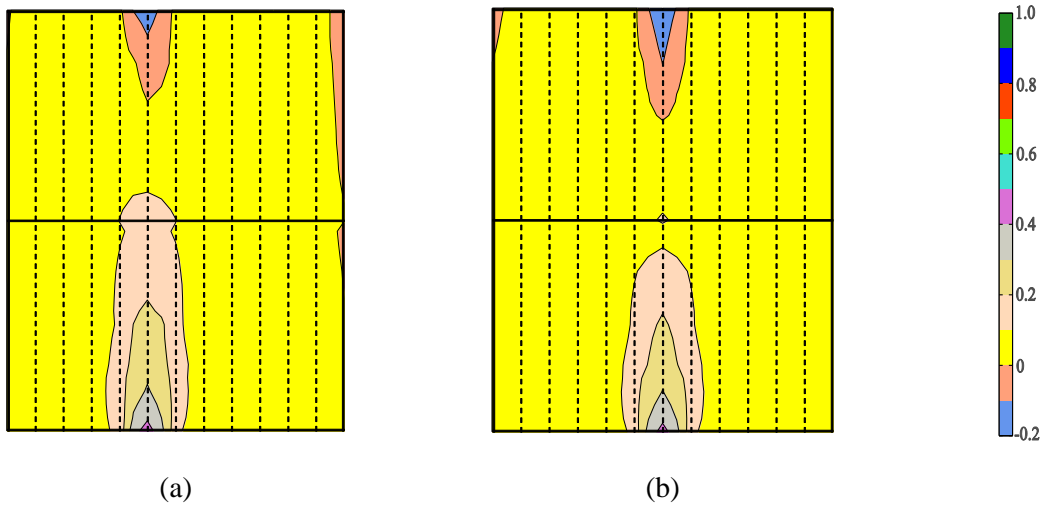


Figure 4. 6: Influence coefficient contours for setup 2 (low RTW stiffness) a) RTW No. 6
b) RTW No. 7

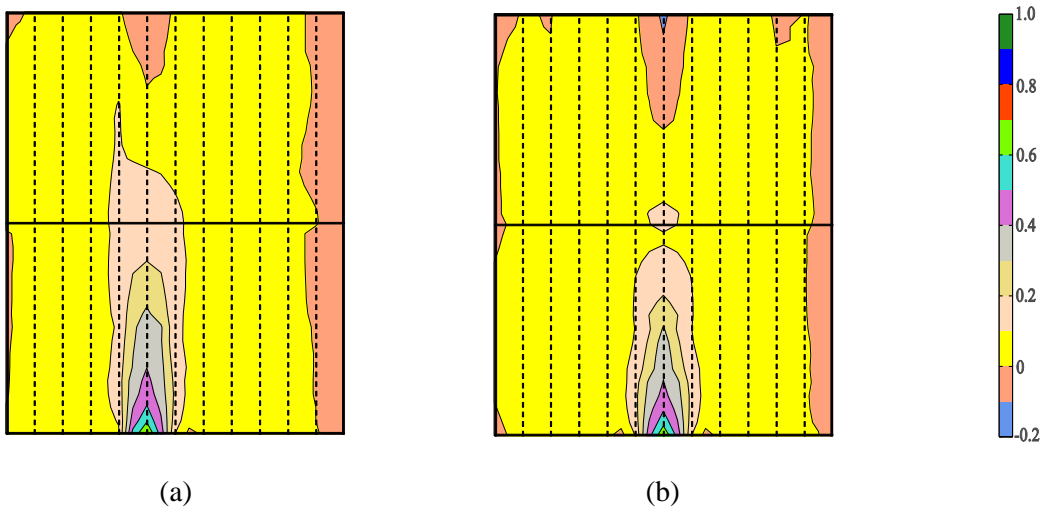


Figure 4. 7: Influence coefficient contours for setup 3 (high RTW stiffness)
a) RTW No. 6 b) RTW No. 7

When the stiffness of RTW connectors is assigned randomly, which is really more indicative of in-situ conditions, the load distribution takes place in proportion to the relative connector stiffnesses. This is addressed in setup 4, the results of which are shown in Figure 4.8. This can be directly compared with Figure 4.2 of setup 1 where the stiffness of all the connectors is constant. The stiffness value of RTW No. 6 is 0.46 kN/mm (2645 lb/in) and of RTW No.7 is 0.68 kN/mm (3856 lb/in), which are both greater than the median value assumed in setup 1 -- 0.37 kN/mm (2126 lb/in). The influence coefficient for RTW No. 6 is 0.68 and RTW No. 7 is 0.75 for setup 4 in comparison to 0.53 and 0.64 respectively of setup 1. Once again, one may see that connector stiffness does affect the localized distribution of load but overall is not largely different than when uniform stiffnesses are utilized.

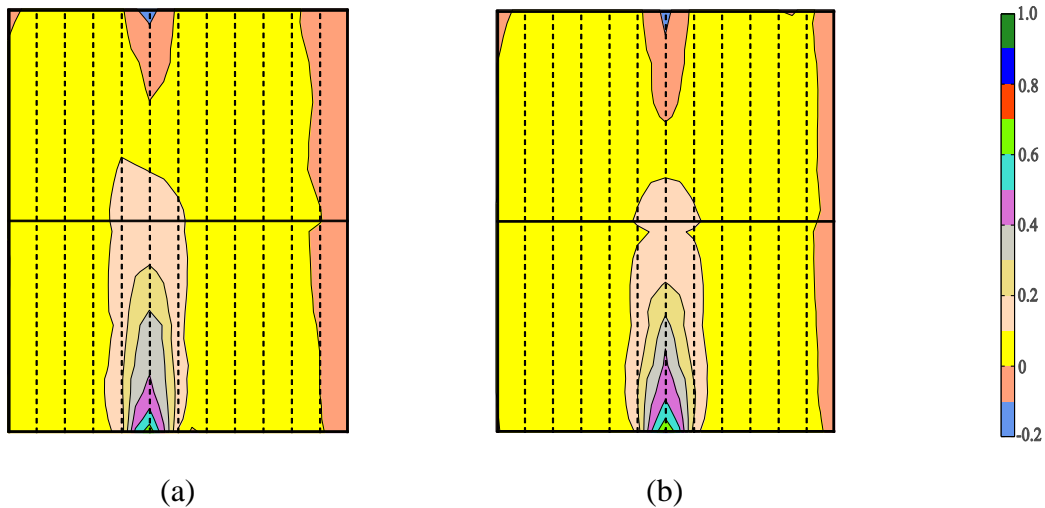


Figure 4. 8: Influence coefficient contours for setup 4 (Random RTW connector stiffness)

a) RTW No. 6 b) RTW No. 7

Setup 5, which is conducted to compare the realistic case of random sheathing connector stiffnesses with the uniform sheathing connector stiffness of setup 1, is shown in Figure 4.9. There is nominally no notable difference between the two scenarios and one may reasonably conclude that there is no need to incorporate this level of randomness into the roof structure modeling of other roofs.

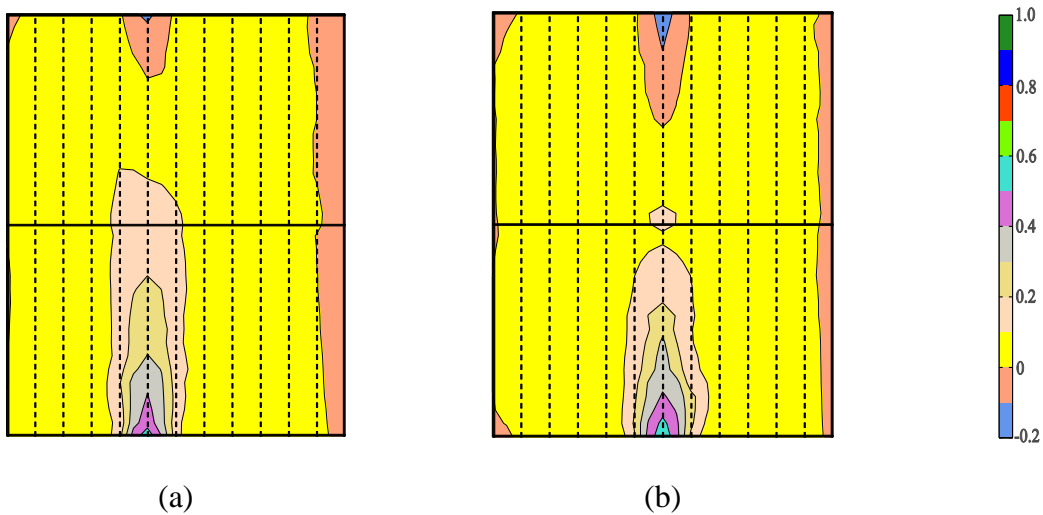


Figure 4. 9: Influence coefficient contours for setup 5 (Random sheathing connector stiffness) a) RTW No. 6 b) RTW No. 7

The effect of sheathing thickness (i.e. stiffness) is demonstrated in Figures 4.10 and 4.11 which show the results for low and high sheathing stiffness respectively. The one with lower sheathing thickness has a slightly narrower influence area than the one with higher sheathing thickness. This confirms with the results obtained by Cramer et al (1989) regarding the load distribution being influenced by the relative stiffness of the sheathing members and truss members but not to a large degree. This reflects the ability of panels to distribute the uplift forces based on the member stiffness.

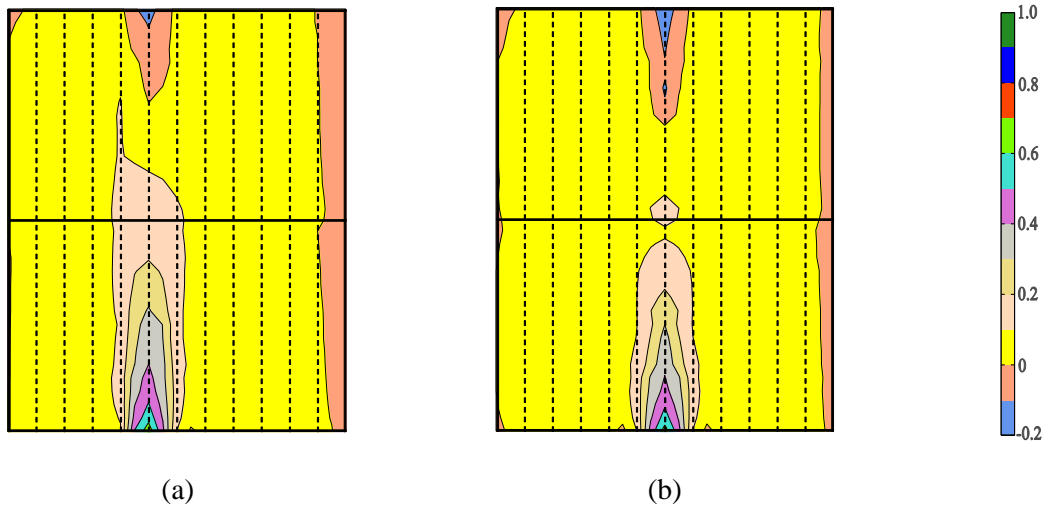


Figure 4. 10: Influence coefficient contours for setup 6 (low sheathing stiffness) a) RTW No. 6 b) RTW No. 7

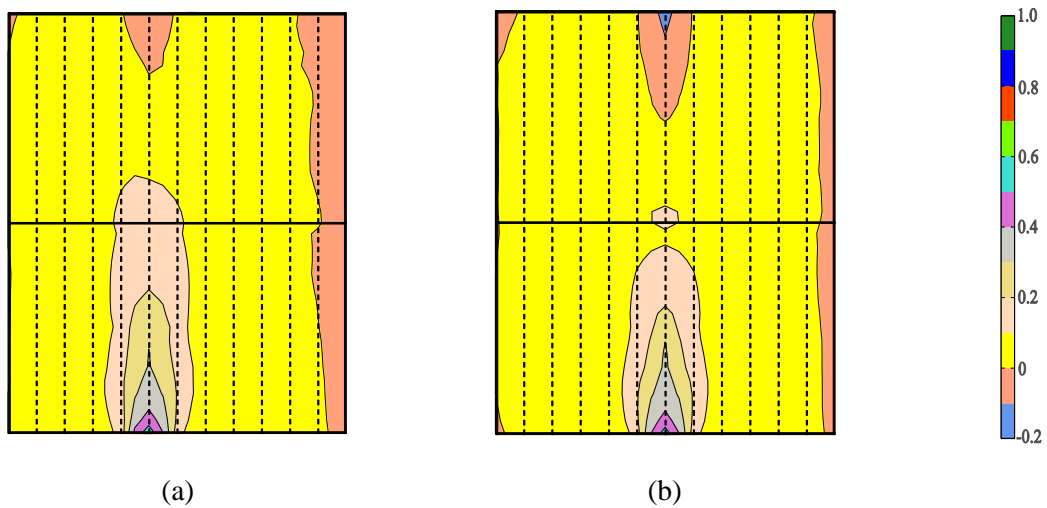


Figure 4. 11: Influence coefficient contours for setup 7 (high sheathing stiffness) a) RTW No. 6 b) RTW No. 7

In Figure 4.12 the effect of having connections between the gable end members and the wall on the influence coefficients can be seen. Only around 40 percent of the load applied over RTW connector number 1 is transferred in setup 1, with gable end members transferring remaining load. Furthermore, the primary influence area is not much greater

than 610 mm (24 in.) x 610 mm (24 in.) square. In contrast the non-presence of gable end members in setup 9 required the RTW connector to now take around 70 percent of the applied load. Incidentally, the area of load distribution would be much higher than in setup 1. An obvious point to be made is that the presence of gable end connections will greatly reduce the probability that RTW number 1 will fail under an extreme wind event. As is well understood, the wind uplift load is the greatest in the region of connector 1 and thus having a reduced influence area will greatly reduce the chance of failure. However, as shown in Figure 4.13, the presence of gable end wall connections has little to no effect on the influence areas of interior RTW connections.

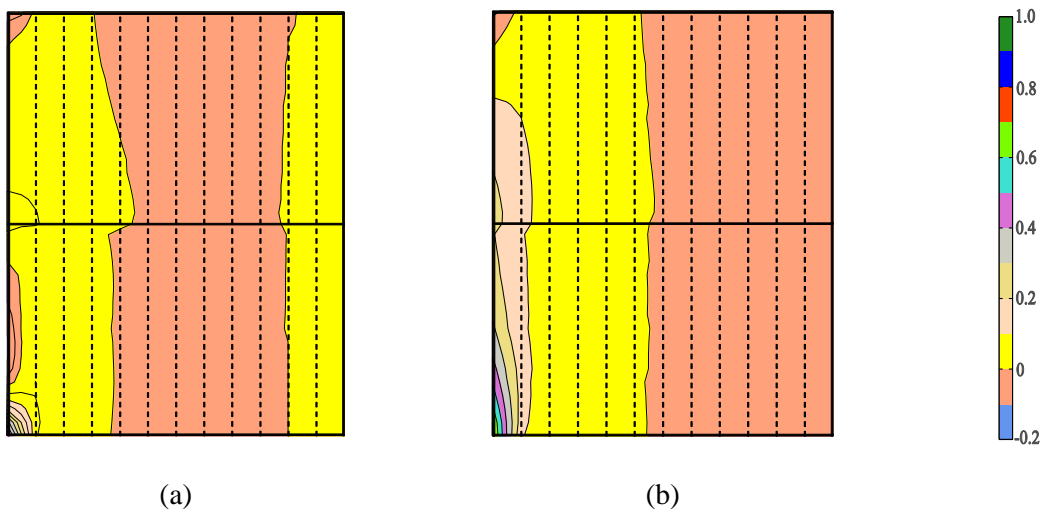


Figure 4. 12: Influence coefficient contours for RTW No. 1 for a) setup 1 (median values) b) setup 9 (no gable connections)

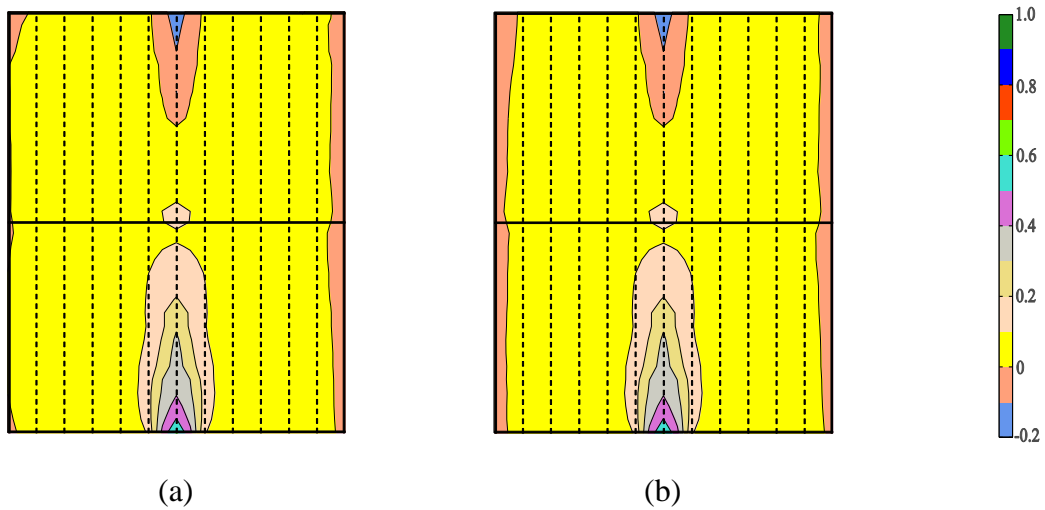


Figure 4. 13: Influence coefficient contours for RTW No. 7 for a) setup 1 (median values) b) setup 9 (no gable connections)

Setup 10 changes the roof framing from trusses to rafters which ultimately impacts the overall and localized stiffnesses of the roof structure. Figure 4.14 should be compared with setup 1 of Figure 4.2 to assess the differences. Though the amount of load transferred when applied above the RTW connector is almost equal, there is a notable reduction in the case of the rafter as the load is applied away from the connector. One may note that the load influence using rafters is much more abbreviated than when using trusses. Load is not easily transferred along the length of the rafter due to the absence of web chords and thus really relies on the localized sheathing transfer mechanism. Another consequence of this is that the rafters spread a slightly higher amount of the applied load to adjacent members when the loading is applied at 1831 mm (72 in.) from the RTW No.7 than that of RTW No.6 (compare with Figures 4.4 and 4.5).

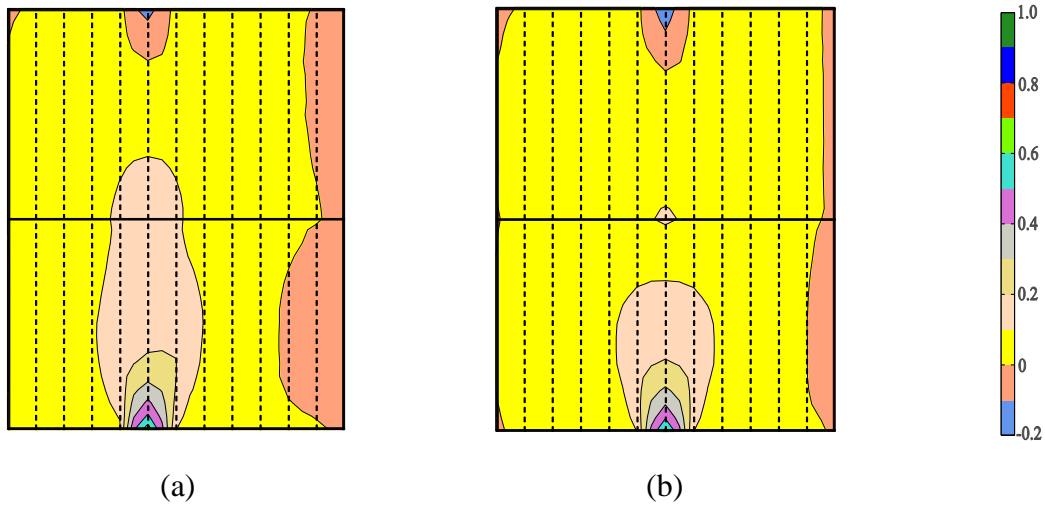


Figure 4. 14: Influence coefficient contours for setup 10 (rafter framing) a) RTW No. 6
 b) RTW No. 7

Nonlinear Behavior Results

For modeling of roof structures under extreme loadings it may become necessary to capture the nonlinear behavior of the connectors. Therefore, a look at the influence coefficients when this nonlinear behavior occurs is of interest to the analyst. This study looked at two additional loading scenarios, one which produces slight localized nonlinearities and one which produces moderate localized nonlinearities. Thus, the uplift load for setup 11 is increased from 0.45 kN (100 lb) to 1.78 kN (400 lb) and for setup 12 the load is set to 3.56 kN (800 lb).

Figure 4.15 shows contours for setup 11 and indicates that very little change, as compared with setup 1, is realized. The coefficient just over the connection is around 60 percent of load applied over that connector. However, as the applied load is increased to that of setup 12, it is observed in Figure 4.16 that only around 30-40 percent of the load applied over the RTW connector gets through to that connector. This change in

distribution is largely due to the yielding of the sheathing connectors to which the load is being applied. Cramer et al. (1989) noted that these sheathing connector failures caused the load to be distributed to adjacent sides of the truss through the sheathing panels.

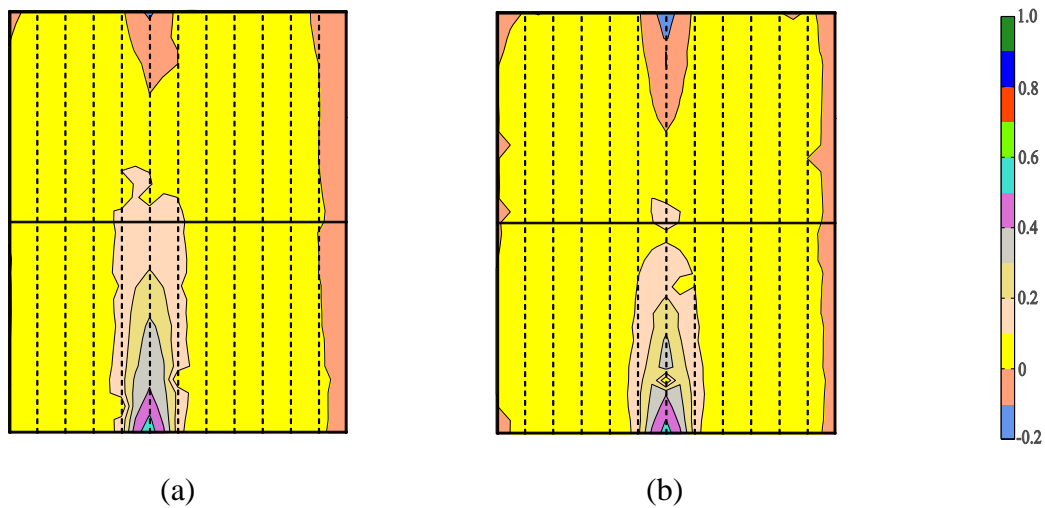


Figure 4. 15: Influence coefficient contours for setup 11 (slight nonlinearity)

a) RTW No. 6 b) RTW No. 7

The magnitude of load applied in both setups 11 and 12 did indeed initiate nonlinear behavior in the connectors. As a result, the irregularities in the contour of Figure 4.16 can be attributed to the non convergence of the analysis when load was applied at certain locations – sheathing panel corners. These analyses were simply removed from the analysis so that the generated contours still capture the general behavior.

With increases in the loading, the normalized reactions of setup 11 remain similar to that of setup 1 (Figure 4.4 and Figure 4.5). Significant changes can be noticed with the

higher load for setup 12. The load applied at RTW No.6 transfers 27 percent of load to the respective connector, 25 percent of load to RTW No.5 and around 30 percent to RTW No.7. The yielding of the sheathing connector causes this difference in load distribution – a consequence of load re-distribution at post-yield. In Figure 4.5 since the RTW no.7 is symmetrical about the sheathing panel, the load transfer remains symmetrical describing the role of sheathing panels in load distribution whereas the same symmetry is not observed in RTW no. 6.

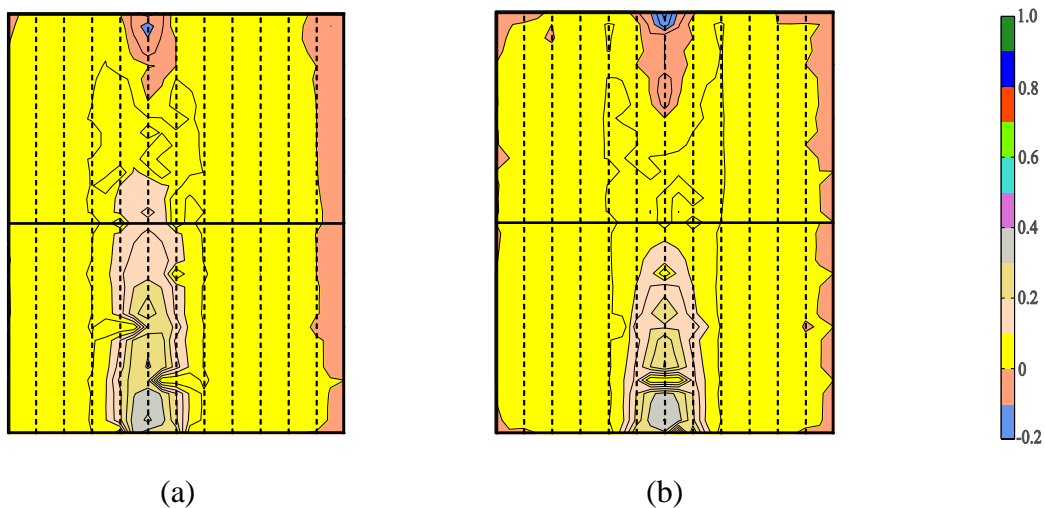


Figure 4. 16: Influence coefficient contours for setup 12 (moderate nonlinearity)

a) RTW No. 6 b) RTW No. 7

To better understand the level of nonlinearity experienced by the connectors, the backbone curves of both the RTW connector no.7 and sheathing connector placed at RTW no.7 are evaluated for a few loading scenarios for setup 12. Figures 4.17 and 4.18 represent the back bone behavior of the RTW and sheathing connector for loads at three different distances from the connector, respectively.

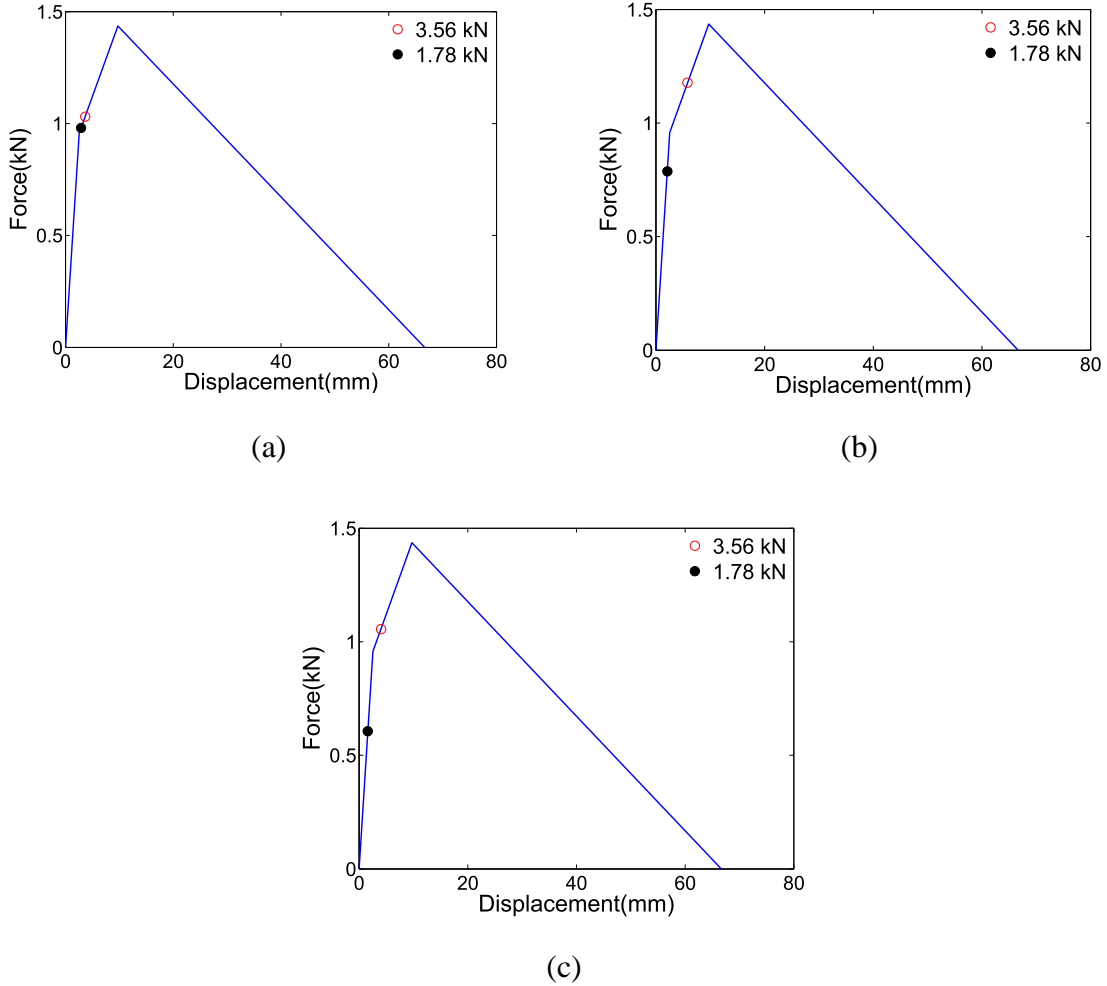
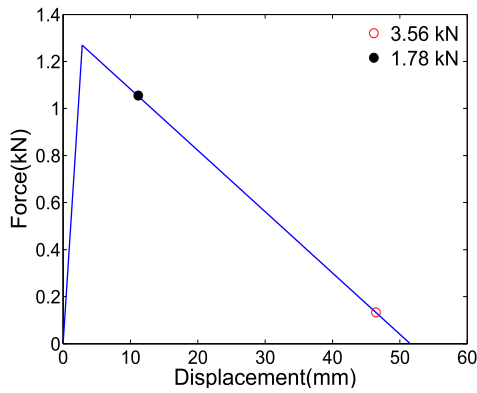


Figure 4. 17: Force displacement behavior of RTW connector no.7 when the load is applied distances a) 0 mm (0 in), b) 610 mm (24 in) and c) 1831 mm (72 in) from RTW No. 7

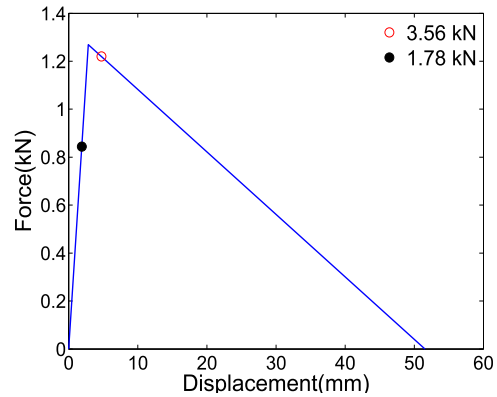
The force displacement curve of the RTW connector no.7 with ultimate force of 1.44 kN (323 lb), the peak load displacement of 9.74 mm (0.38 in.) and the ultimate displacement of 66.68 mm (2.63 in.) is utilized to check the connector properties when the analysis is completed. In Figure 4.17 a. the uplift force in the connector has increased slightly beyond the linear range for both the 1.78 kN (400 lb) and 3.56 kN (800 lb) with

the value of force being 0.98 kN (220 lb) and 1.03 kN (231 lb) respectively. However the force in the connector has not reached the ultimate uplift force.

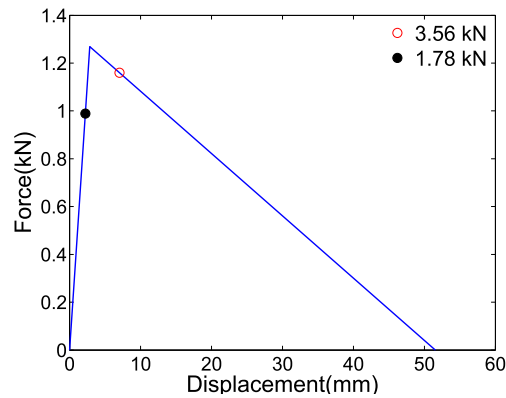
When the loading is placed further away from the connector, the case with loading 1.78 kN (400 lb) remains in the linear range whereas in the 3.56 kN (800 lb) case it goes well into the nonlinear stage. As the distance between the point of load application and the RTW connector increases, the internal force experienced by the connector due to load distribution decreases for the lower level of load application - 1.78 kN (400 lb). However, this same phenomenon is not entirely true for the case of the larger load application - 3.56 kN (800 lb). An examination of Figures 4.17b and 4.17c actually shows that the load in the connector increases as the distance between the load and the connector increases. This is because of the sheathing connectors acting as a fuse. As the sheathing connector yields, the system relies more and more on the sheathing to handle the distribution of load. This tends to have a smoothing effect on the load distribution.



(a)



(b)



(c)

Figure 4. 18: Force displacement behavior of sheathing connectors at distances

a) 0 mm (0 in), b) 610 mm (24 in) and c) 1831 mm (72 in) from RTW No. 7 when load placed over respective connectors.

Sheathing connectors encounter similar behaviors as the RTW connectors do due to higher loadings. Moreover, sheathing connectors form the higher order members in transferring the load to the foundation making them experience greater effect than the RTW connectors. It often leads to the complete withdrawal of the connectors. The backbone curve of sheathing connector is defined with an ultimate force of 1.27 kN

(285.43 lb) and an ultimate displacement of 51.56 mm (2.03 in.) The sheathing connectors at the RTW No.7 remained in the post ultimate force (nonlinear) range for both load cases (Figure 4.18 a). The connectors placed at 609 mm (24 in.) and 1831 mm (72 in.) (Figure 4.18 b. and c.) away from the RTW connector no.7 remains in the nonlinear range when higher load is applied. This of course indicates that a load redistribution must be carried out to be able to adequately handle the load.

CHAPTER FIVE

CONCLUSIONS

This study looks to enhance the present understanding of the factors which influence the way loads are distributed in LFWR structures. This is done by performing a sensitivity study of load influence coefficients subjected to various modeling parameters such as connection stiffness, sheathing stiffness, framing type and nonlinear behavior. The FE model developed as part of this analytical research work effectively predicted the load path of the LFWR system. Influence coefficients were developed for uplift and gravity loads for various RTW connections.

Several conclusions can be drawn from this study which includes:

- The direction of loading has an appreciable influence on the load paths. Influence coefficients illustrate the difference in the way loads are distributed through the system through comparison of uplift and gravity type loads. The difference in the magnitude of load transferred to connections for gravity loads compared to uplift load can reach as high as 30 - 40 percent. This change is due to the large difference between connector stiffnesses in compression and tension. Thus, if models are to be generated for analyzing wind effects, the traditionally used pin connections at the RTW interface may not be appropriate for capturing the true system response.

- The stiffness of the connectors emphasizes the importance of load distribution with connectors having higher stiffness carrying more load than the connectors with lower stiffness. The staggered sheathing panels contribute in resisting the uplift load by more effectively distributing the load to adjacent trusses. This reduces the effects of the weak link created at a single location due to extreme winds as evidenced by the nonlinear portion of this study.
- Since the sheathing is the mechanism by which loads are distributed, the relative stiffness of sheathing to framing and connectors can affect how loads are distributed. The low sheathing stiffness requires a single RTW connector to carry a higher share of the load applied directly over it.
- The intermediate truss-to-wall connections along the gable end truss add many more possible load paths which has the net effect of reducing the load carried by the connections at the truss heel. However, the benefit of these connections are really only felt at the gable and penultimate trusses. Hence, the heels at these trusses can have smaller RTW connectors leading to a slightly lower construction cost as long as the intermediate connectors are capable of resisting the requisite uplift forces.
- As sheathing connectors and/or the RTW connectors begin to yield, the sheathing will tend to redistribute the load to adjacent trusses. This stresses again the significance which connector stiffness plays in the distribution of loads.

- The modeling of sheathing panels as shell elements, rather than creating them as equivalent beam elements, and explicitly modeling of sheathing connectors helps to better understand the true nature of the load distribution in a roof system.
- The tributary area of a RTW connector extends to just over one adjacent truss spacing on either side of the connector. However, this influence area can increase as the connector stiffness reduces. If the connector is being designed for a distributed load, the traditional tributary approach for calculating design forces appears to be sufficient. However, if the connector is being design for more of a localized set of forces, the tributary approach will likely underestimate the design forces. Such an impact on design decisions has also been highlighted by LaFave et al. (1992).
- The findings of the study provide a basis on which a simplified fragility analysis methodology may be developed for these types of roofs. An analyst may not be required to analytically model each and every connector and piece of framing but rather may simply use the influence areas to assign demand forces to the connectors. This further corroborates the findings in a recent fragility based study of a similar roof system (Shanmugam 2011).

REFERENCES

- ANSYS. (2009). "ANSYS users manual; version 12.0 : 2009" ANSYS, Inc., Canonsburg, PA.
- Baskaran, A., and Dutt, O. (1997). "Performance of roof fasteners under simulated loading conditions." *Journal of Wind Engineering and Industrial Aerodynamics*, 72, 389-400.
- Cramer, S. M., and Wolfe, R. W. (1989). "Load-distribution model for light-frame wood roof assemblies." *Journal of Structural Engineering*, 115(10), 2603-2616.
- Cramer, S. M., Drozdek, J. M., and Wolfe, R. W. (2000). "Load sharing effects in light-frame wood-truss assemblies." *Journal of Structural Engineering*, 126(12), 1388-1394.
- Dao, T. N. and van de Lindt, J.W. (2008). "New nonlinear roof sheathing fastener model for use in finite-element wind load applications." *Journal of Structural Engineering* 134(10): 1668-1674.
- Datin, P.L., Mensah, A.F., and Prevatt, D.O. (2008). "Experimentally determined structural load paths in a 1/3-scale model of light-framed wood, rectangular building."
- Datin, P.L. (2010). "Structural load paths in low-rise, wood-framed structures". Ph.D. Thesis, University of Florida, Gainesville, FL.
- Doudak, G. (2005). "Field determination and modeling of load paths in wood lightframe structures." Ph.D. Thesis, McGill University, Montreal, Quebec, Canada.
- Edmonson, W.C., Schiff, S.D. and Nielson, B.G. (2011). "Behavior of light-framed wood roof-to-wall connectors using aged lumber and multiple connection mechanisms", *Journal of Performance of Constructed Facilities*, (In Press).
- Gupta, R. (2005). "System Behavior of Wood Truss Assemblies." *Progress in Structural Engineering and Materials*, 7(4), 183-193.
- Gupta, R. and Limkatanyoo, P. (2008). "Practical Approach to Designing Wood Roof Truss Assemblies." *Practice Periodical on Structural Design and Construction*, 13(3):135-146.
- LaFave, K.D. and Itani, R.Y. (1992). "Comprehensive Load Distribution Model for Wood Truss Roof Assemblies." *Wood and Fiber Science (SWST)*, 24(1), 79-88.

- Li, Z., Gupta, R., and Miller, T. H. (1998). "Practical approach to modeling of wood truss roof assemblies." *Practice Periodical on Structural Design and Construction*, 3(3), 119-124.
- Liu, W.-F., and Bulleit, W. M. (1995). "Overload behavior of sheathed lumber systems." *Journal of Structural Engineering*, 121(7), 1110-1118.
- Mani, S. (1997). "Influence Functions for Evaluating Design Loads on Roof-Truss to Wall Connections in Low-Rise Buildings," M.S. Thesis, Clemson University, Clemson, SC.
- Martin, K. G. (2010). "Evaluation of system effects and structural load paths in a wood-framed structure," MS Thesis, Oregon State University, Corvallis, OR.
- Melchers, R.E (2001). *Structural reliability analysis and prediction*, second ed. West Sussex (England): John Wiley & Sons Ltd.
- Reed, T. D., Rosowsky, D. V., and Schiff, S. D. (1997). "Uplift capacity of light-frame rafter to top plate connections." *Journal of Architectural Engineering*, 3(4), 156-163.
- Shanmugam, B., Nielson, B. G., and Prevatt, D. O. (2008). "Probabilistic descriptions of in-situ roof to top plate connections in light frame wood structures." *Proceedings of the 2008 Structures Congress - Structures Congress 2008: Crossing the Borders*, American Society of Civil Engineers, Vancouver, BC, Canada.
- Shanmugam, B., Nielson, B.G., Prevatt, D.O. (2009). "Statistical and analytical models for roof components in existing light-framed wood structures."
- Shanmugam, B. (2011) "Probabilistic assessment of roof uplift capacities in low-rise residential construction". Ph.D. Thesis, Clemson University, Clemson, SC.
- Shirazi, S.M.H., and Pang, W. (2011). "Propagation of Aleatoric Uncertainty in Light-frame Wood Shear Walls", 11th International Conference on Applications of Statistics and Probability in Civil Engineering) August 1- 4, 2011, ETH Zurich, Switzerland (In Press).
- Silva, A. and Gesualdo, F. A. R. (2005). "Numerical analysis of the boundary conditions of wooden shear walls in the light platform system." *Asian Journal of Civil Engineering (Building and Housing)*, Vol. 6, No. 3:113-126.

Taly, N. (2003). *Loads and Load Paths in Buildings: Principles of Structural Design*. International Code Council, Inc., IL.

US Census Bureau. (2010). "Population Estimates. US Dept. of Commerce: 2010."

US Census Bureau. (2010). "2010 Population Estimates." US Dept. of Commerce, Economics and Statistics Administration, Washington, D.C., Accessed 3/21/2011 from factfinder.census.gov.

Van de Lindt, J.W., Graettinger, A., Gupta, R., Skaggs, T., Pryor, S., and Fridley, K. (2007). "Performance of Wood frame Structures During Hurricane Katrina." *Journal of Performance of Constructed Facilities*, 21(2), 108-116.

Wolfe, R. W. and LaBissoniere, T. (1991). "Structural Performance of Light-Frame Roof Assemblies II. Conventional Truss Assemblies." FPL-RP-499, Forest Products Laboratory, Madison, WI.

APPENDIX A

INFLUENCE COEFFICIENT CONTOURS

This appendix provides the influence coefficient contours for all of the 12 setups. Since the contours of roof-to-wall (RTW) connectors of both ends of the truss are symmetrical, contours for the left support of all the 13 trusses and for the connector provided below the ridge of the gable end truss is provided. The scale shown in Figure A.1 shall be referred for all the contours.

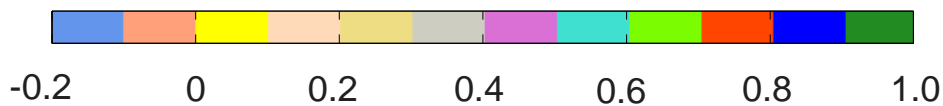


Figure A. 1: Influence coefficient scale

In each of the following figures, the influence coefficient contour of

- a. RTW connector at center of gable truss
- b. RTW connector no.1
- c. RTW connector no.2
- d. RTW connector no.3
- e. RTW connector no.4

- f. RTW connector no.5
- g. RTW connector no.6
- h. RTW connector no.7
- i. RTW connector no.8
- j. RTW connector no.9
- k. RTW connector no.10
- l. RTW connector no.11
- m. RTW connector no.12
- n. RTW connector no.13

In setup 1, the average stiffness values of both RTW and sheathing connectors are considered. The sheathing thickness is assumed to be 11.9 mm (15/32 in.) which is regarded as the median thickness. The model is generated with interior trusses in fink style with gable end members pin supported on wall. An uplift load of 0.45 kN (100 lbs) is then used to analyze the model.

In setup 2, the lower stiffness value from Table 3.1 is used to define withdrawal behavior of the RTW connectors. Likewise, the higher stiffness value for setup 3 and

random values for all 26 connectors in setup 4 are defined. The remaining inputs remained the same as in setup 1.

The influence of sheathing connector stiffness is investigated in setup 5. This looks at the case where each sheathing connector can have a different initial stiffness as opposed to all having the same stiffness as done in setup 1. The effect of sheathing stiffness is then evaluated in the next two setups where sheathing thickness is changed to 9.5 mm (0.375 in.) in setup 6 and to 15.9 mm (0.625 in.) in setup 7.

Setup 8 reverses the direction (noted as a gravity case) of the applied load such that all RTW connectors are placed in compression rather than the tension which typically results from uplift loads. The stiffness of RTW connections in compression is very high because the truss bears directly on a wall. However, in tension the stiffness is relatively low because only the toe-nails are providing any resistance. In short, the connection behaves as a pin connection in the gravity case and an elastic support in all other setups.

The impact of the gable end wall connections on load influence is investigated in setup 9 while relative framing stiffness, implemented in the form of different framing schemes, is examined in setup 10. Finally, the change in load influence as the connection behavior begins to go nonlinear is explored in setups 11 and 12 where the applied uplift load is set at 1.78 kN (400 lbs) and 3.56 kN (800 lbs) respectively.

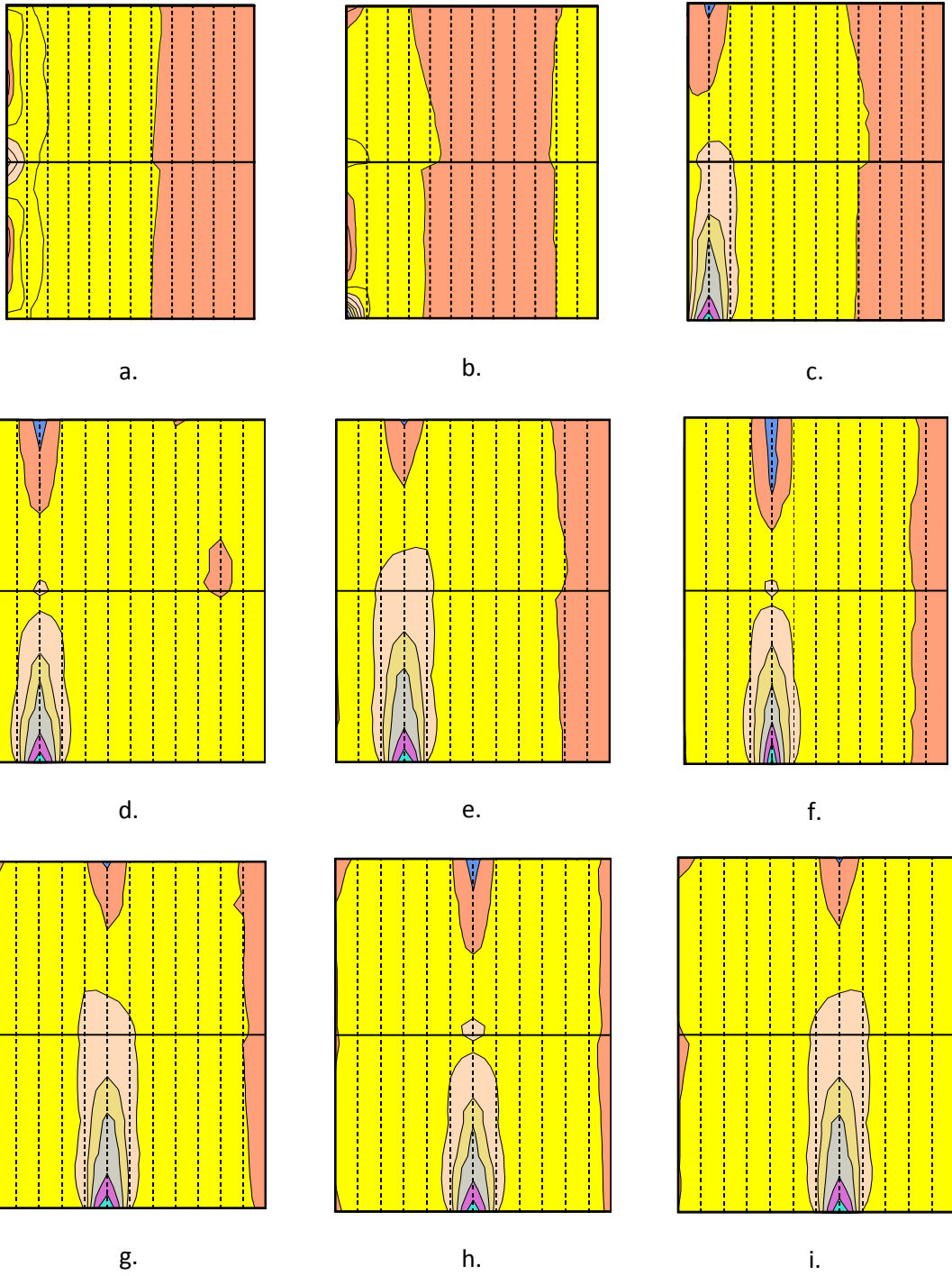
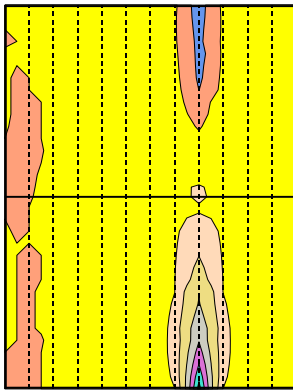
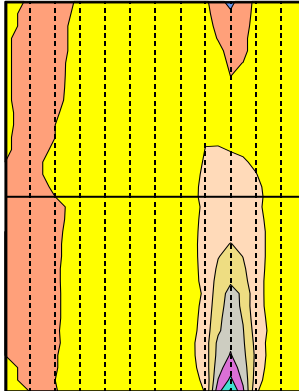


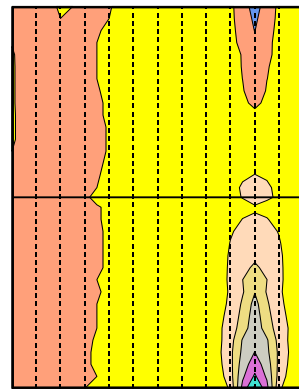
Figure A. 2: Influence coefficient contours for setup 1



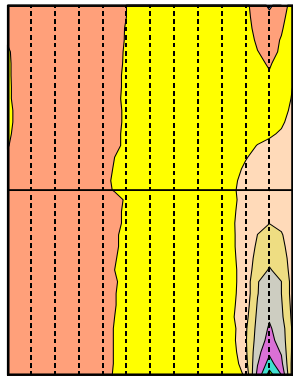
j.



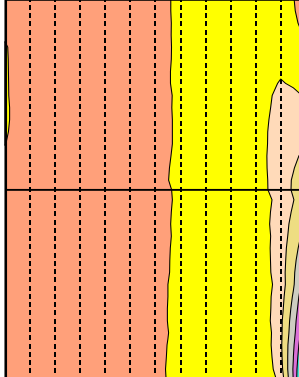
k.



l.



m.



n.

Figure A. 3: Influence coefficient contours for setup 1(contd.)

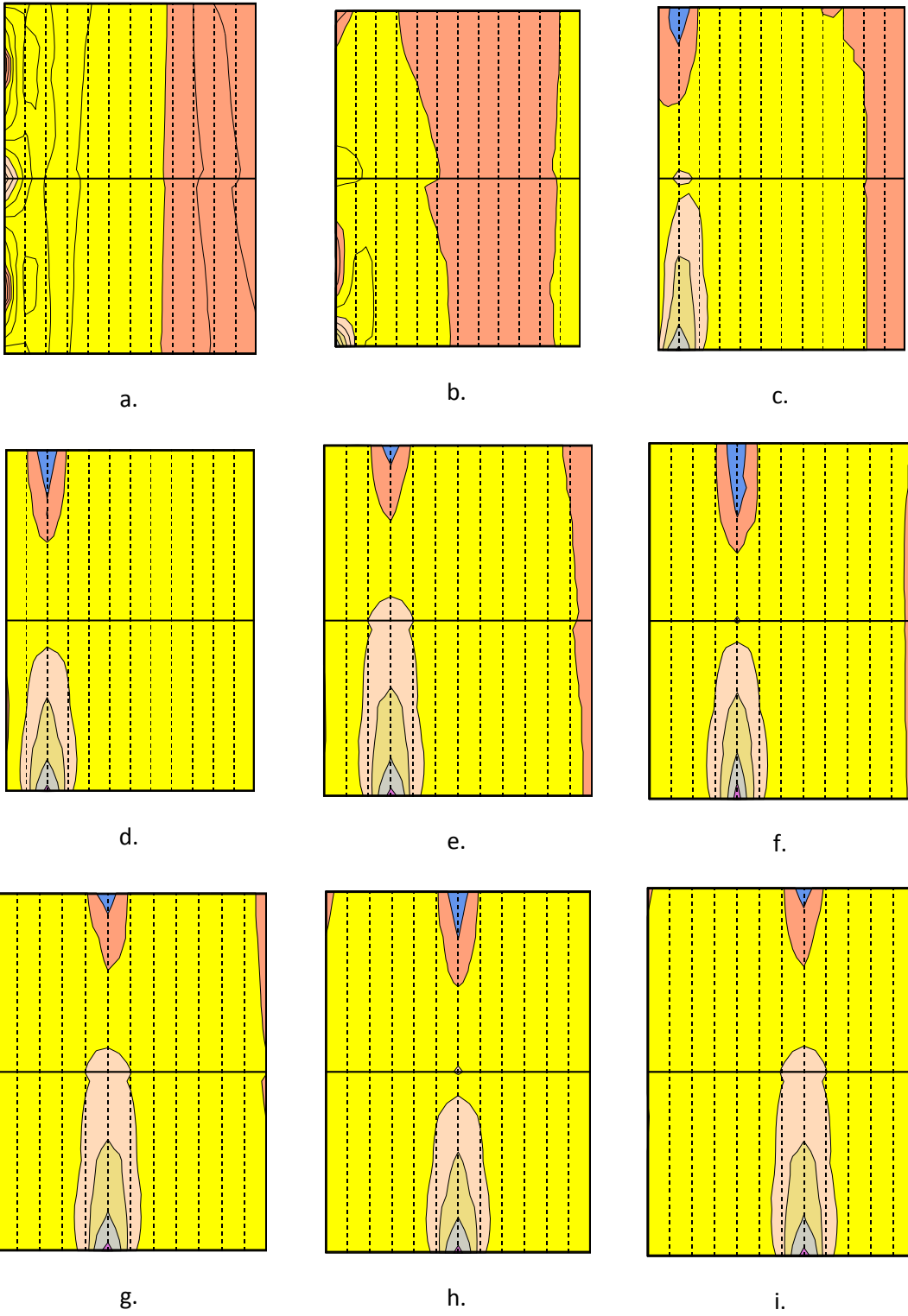
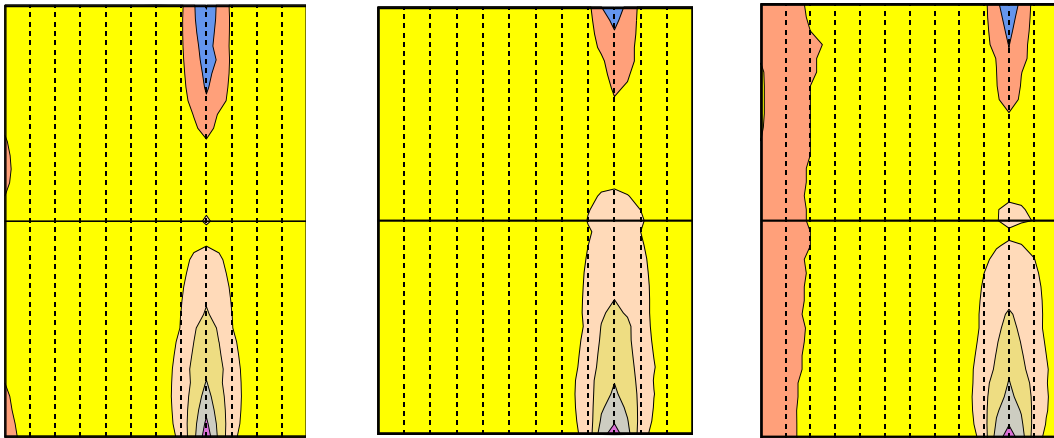


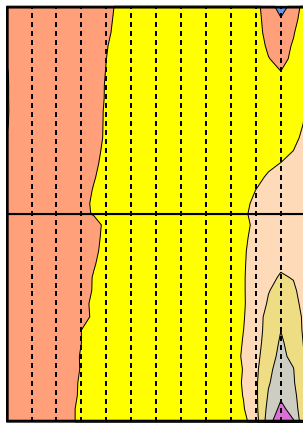
Figure A. 4: Influence coefficient contours for setup 2



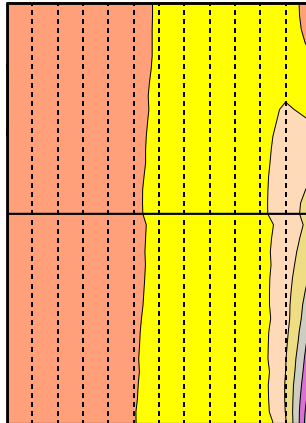
j.

k.

l.

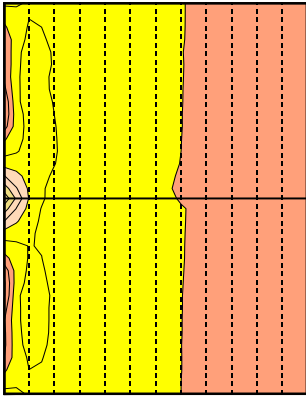


m.

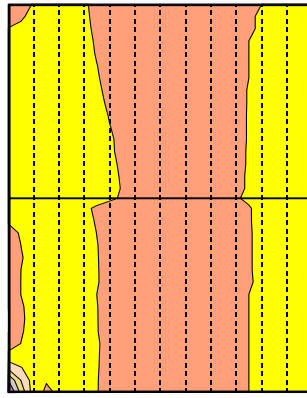


n.

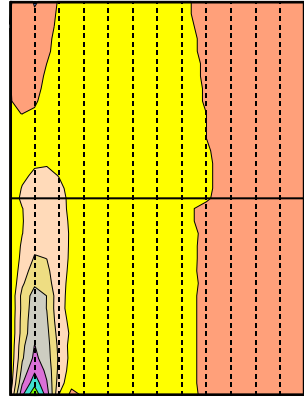
Figure A. 5: Influence coefficient contours for setup 2(contd.)



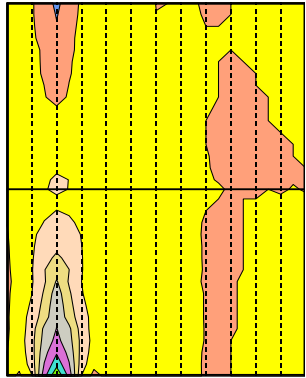
a.



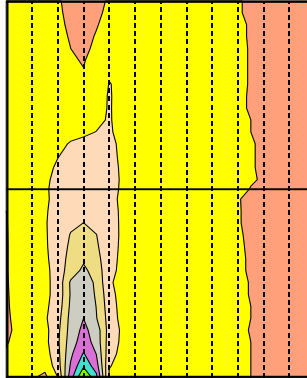
b.



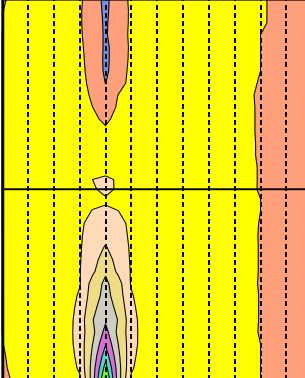
c.



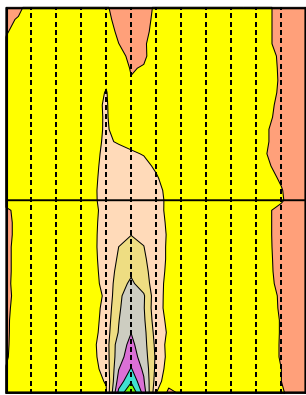
d.



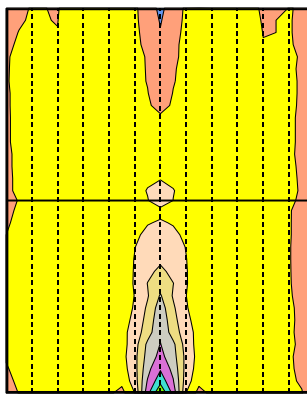
e.



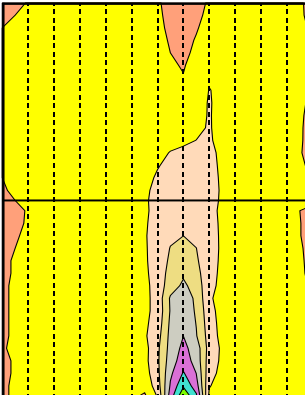
f.



g.

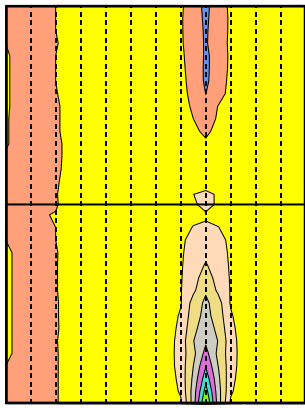


h.

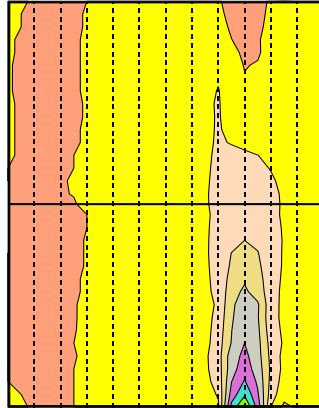


j.

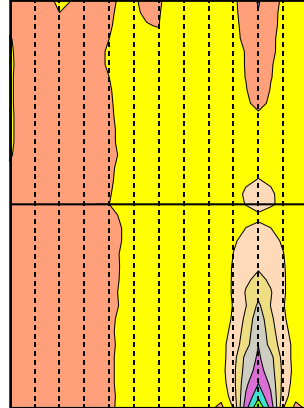
Figure A. 6: Influence coefficient contour for setup 3



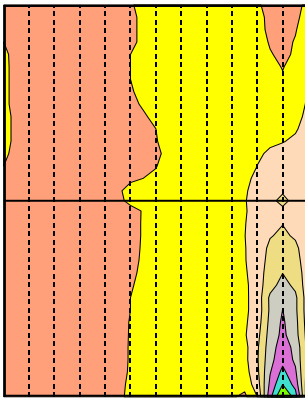
j.



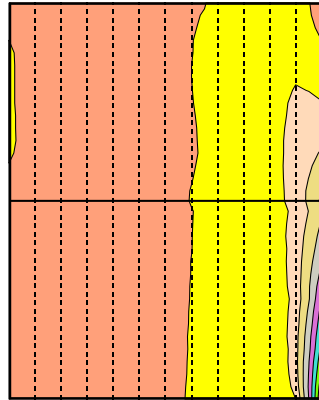
k.



l.



m.



n.

Figure A. 7: Influence coefficient contour for setup 3(contd.)

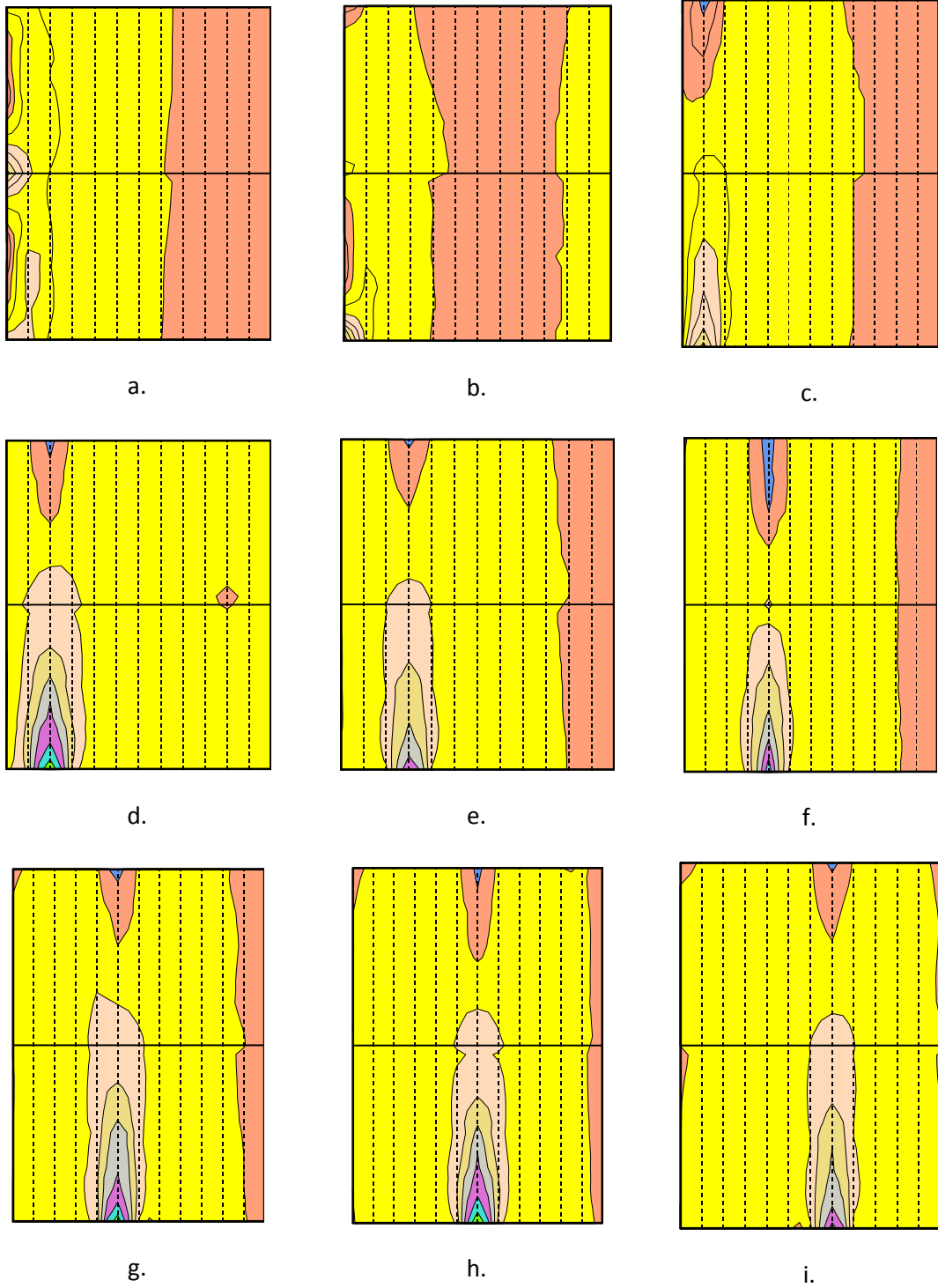
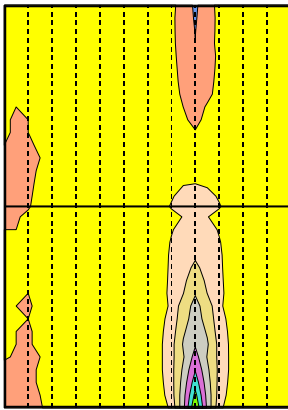
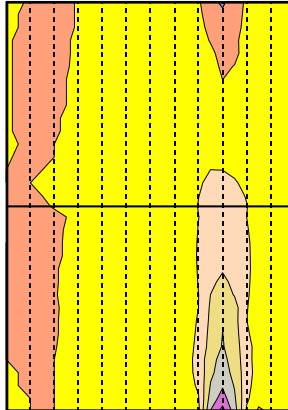


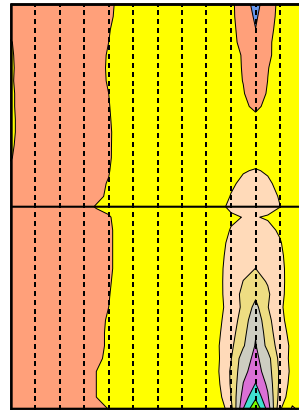
Figure A. 8: Influence coefficient contour for setup 4



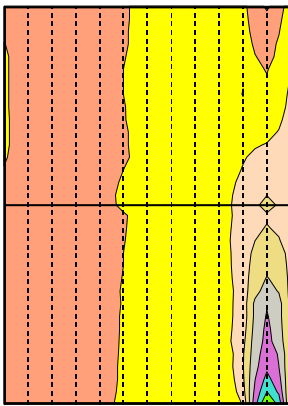
j.



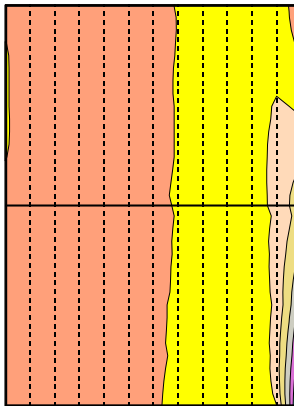
k.



l.



m.



n.

Figure A. 9: Influence coefficient contour for setup 4(contd.)

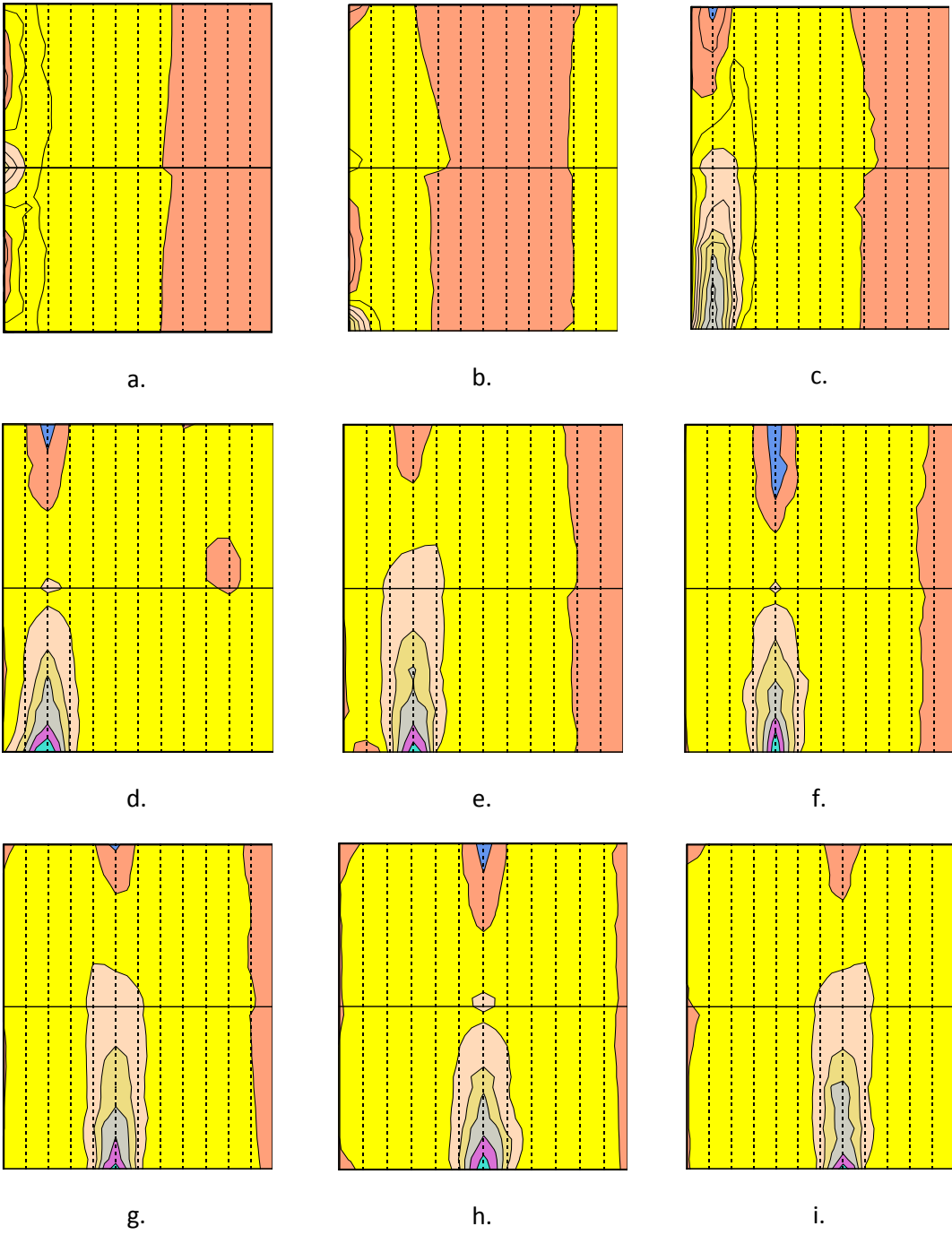


Figure A. 10: Influence coefficient contour for setup 5

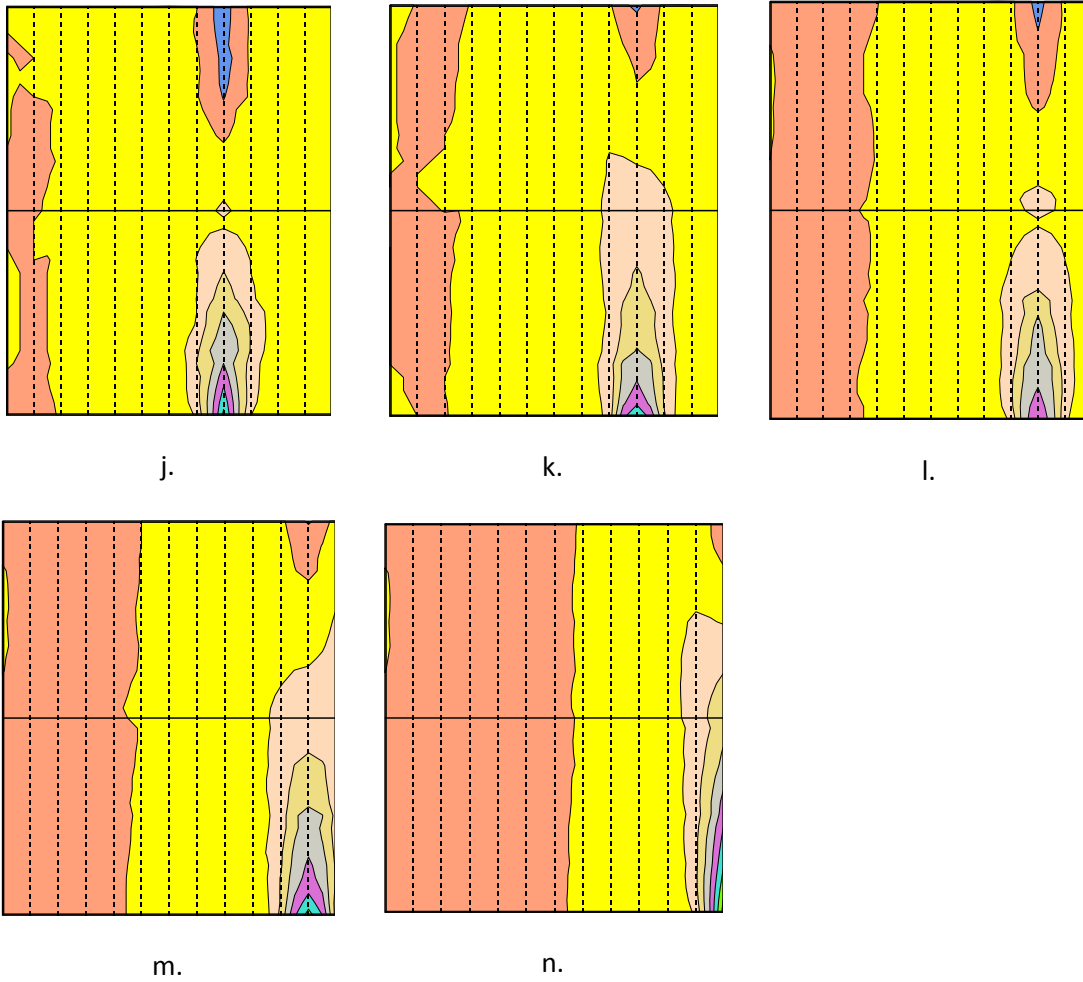


Figure A. 11: Influence coefficient contour for setup 5(contd.)

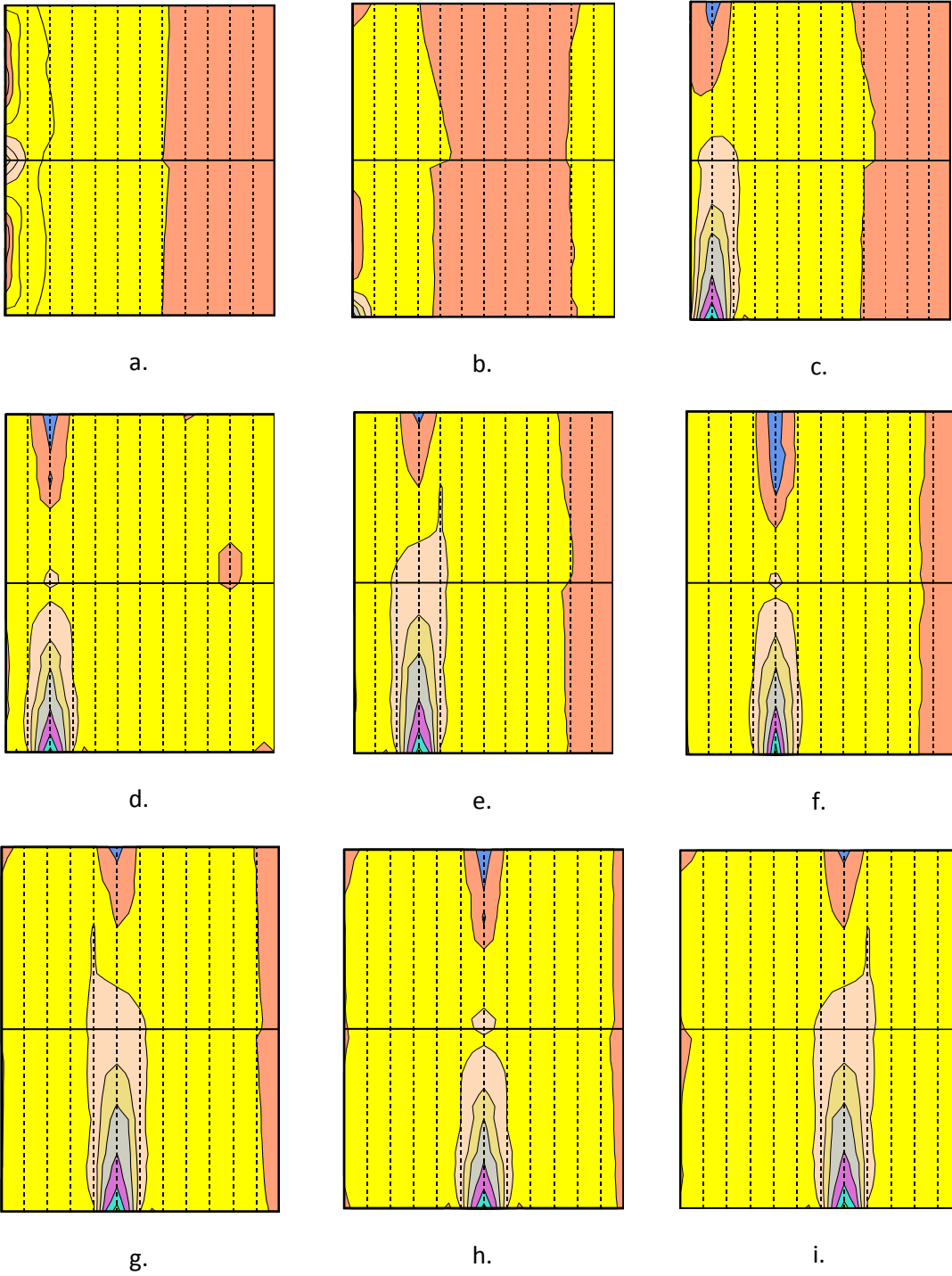
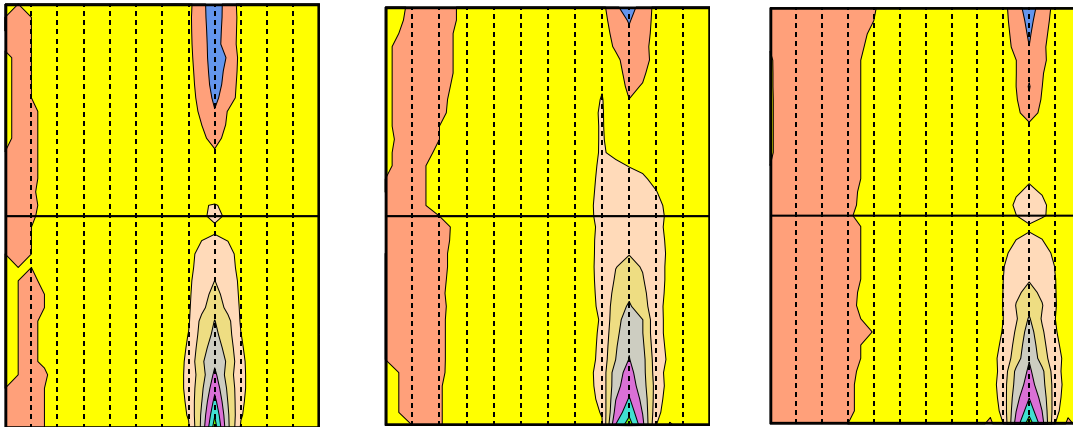


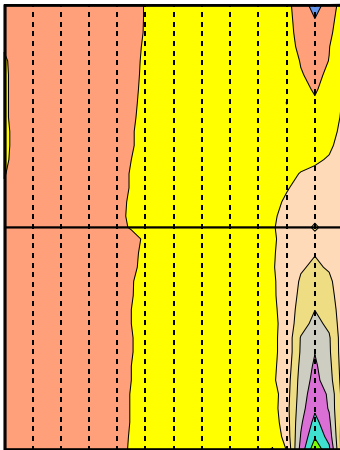
Figure A. 12: Influence coefficient contour for setup 6



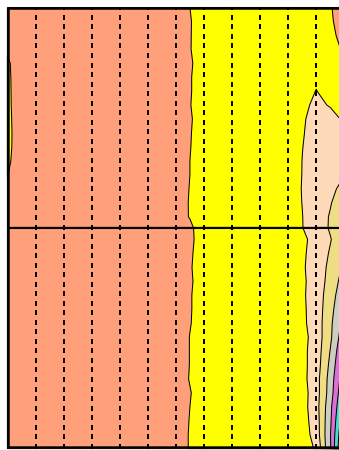
j.

k.

l.



m.



n.

Figure A. 13: Influence coefficient contour for setup 6(contd.)

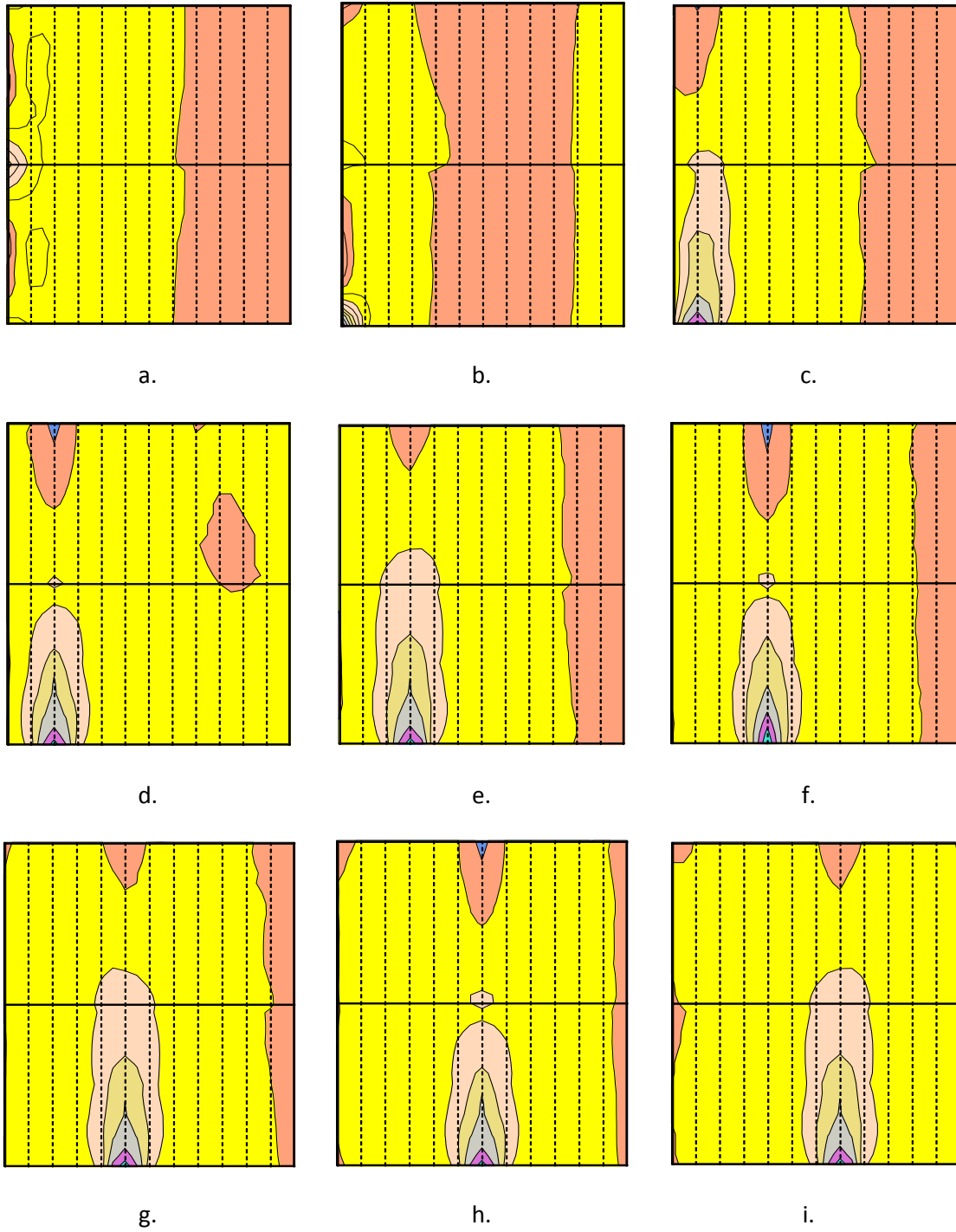
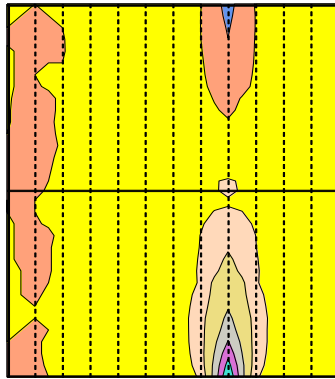
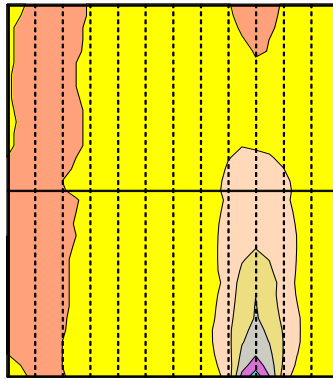


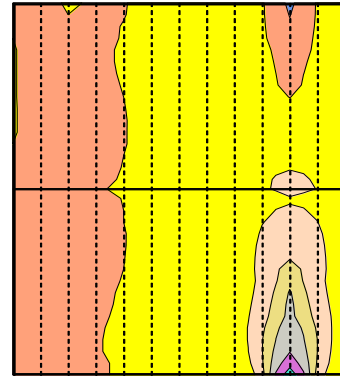
Figure A. 14: Influence coefficient contour for setup 7



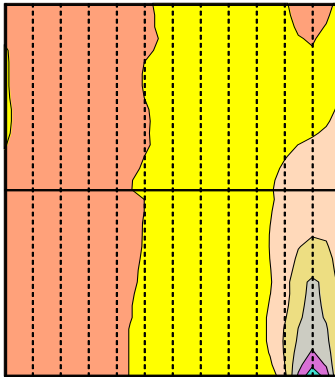
j.



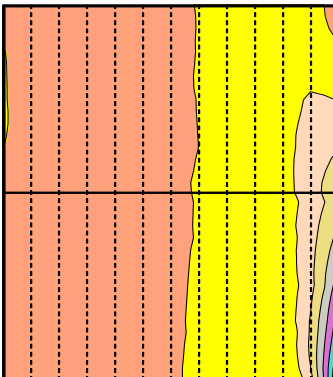
k.



l.



m.



n.

Figure A. 15: Influence coefficient contour for setup 7(contd.)

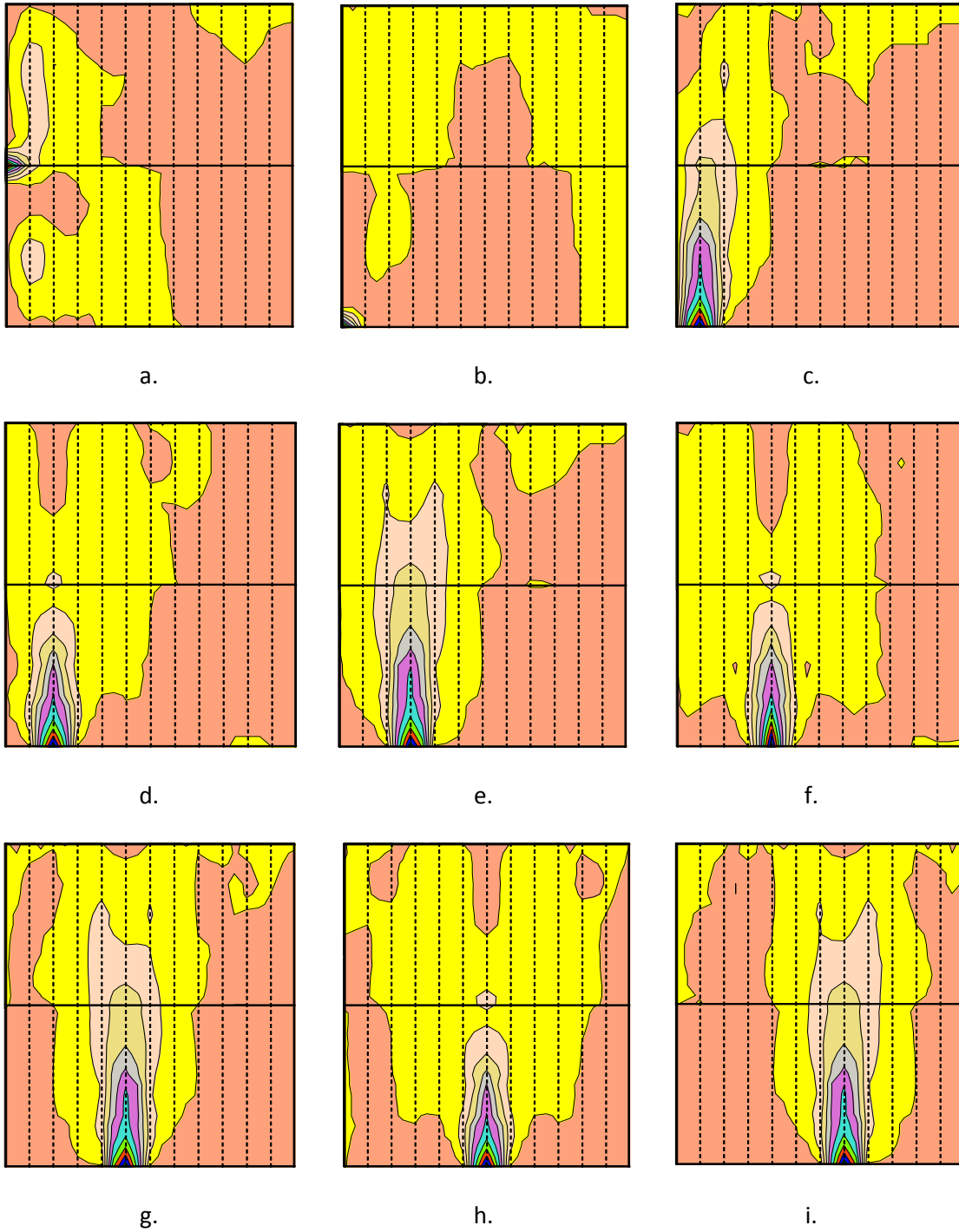
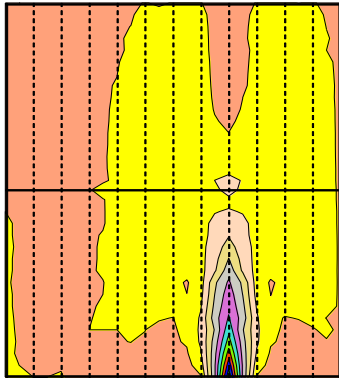
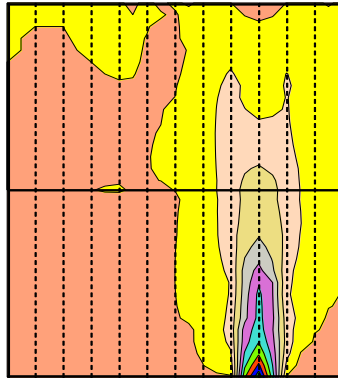


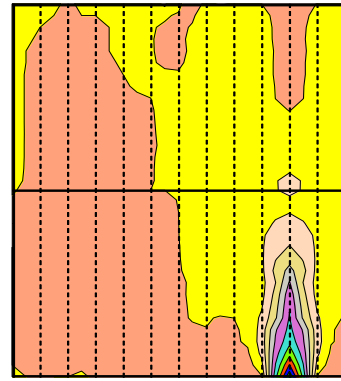
Figure A. 16: Influence coefficient contour for setup 8



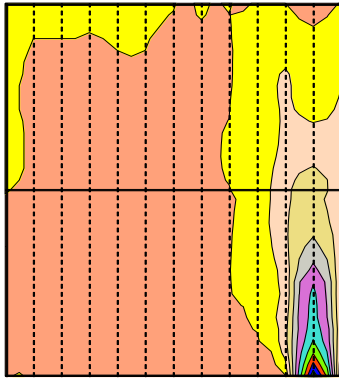
j.



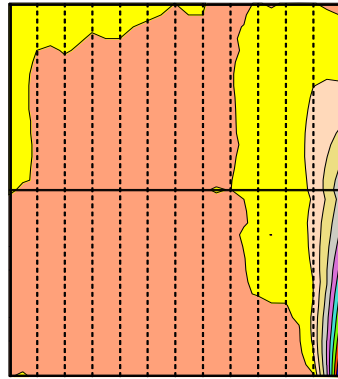
k.



l.



m.



n.

Figure A. 17: Influence coefficient contour for setup 8(contd.)

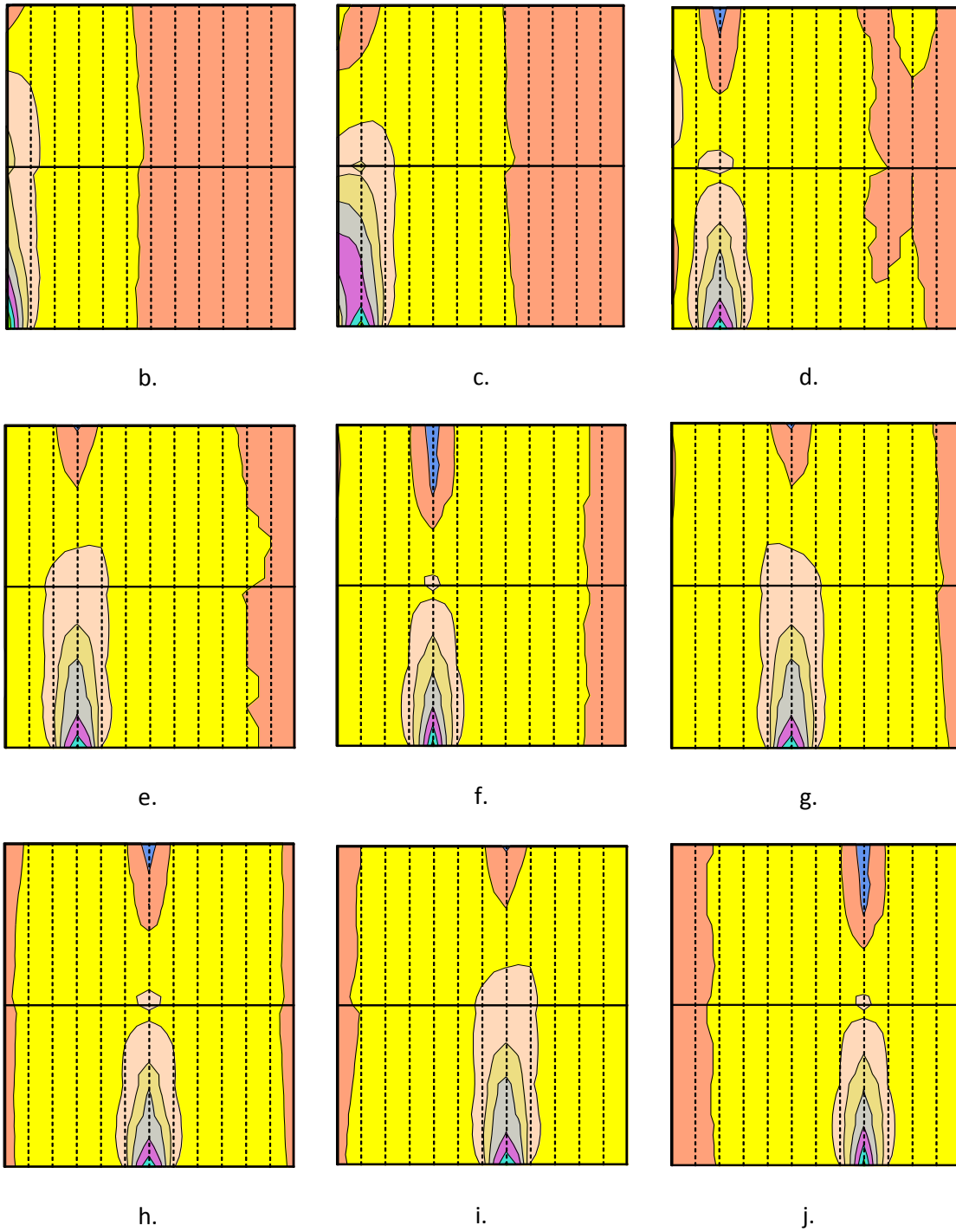
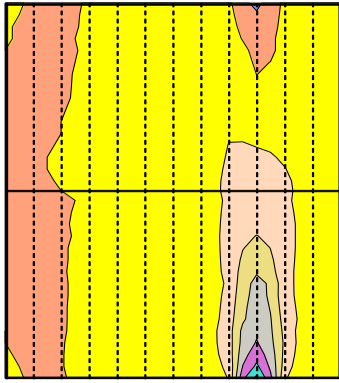
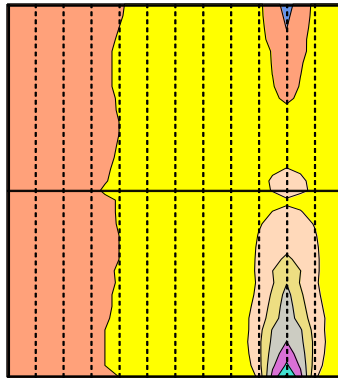


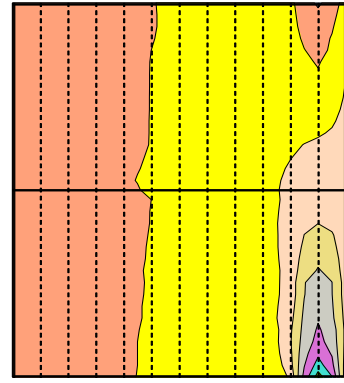
Figure A. 18: Influence coefficient contour for setup 9



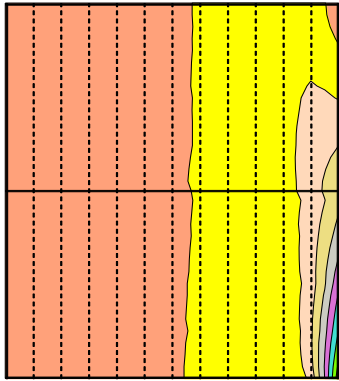
k.



l.



m.



n.

Figure A. 19: Influence coefficient contour for setup 9(contd.)

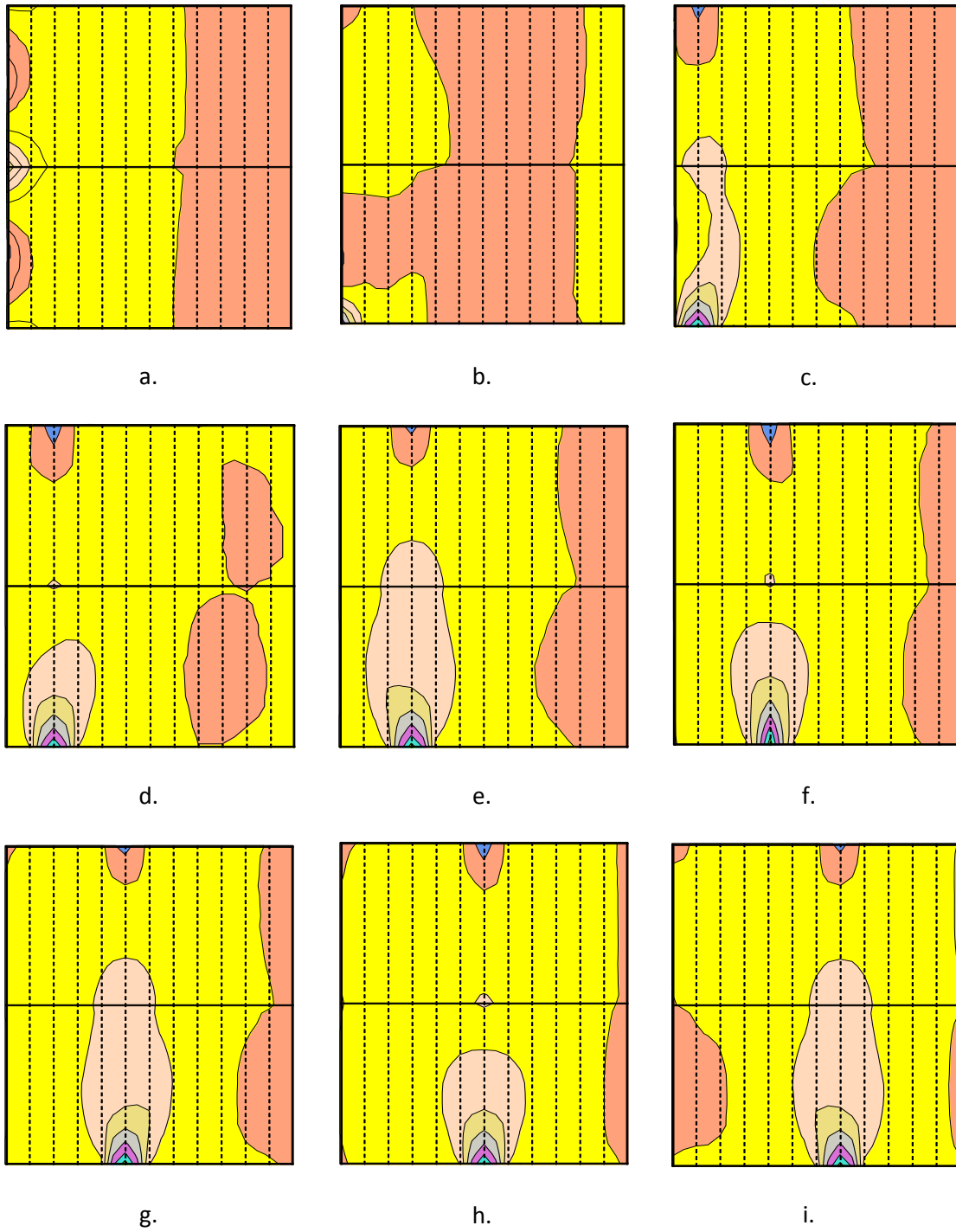
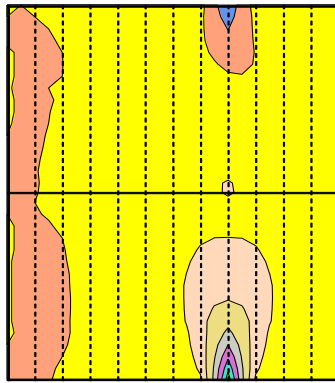
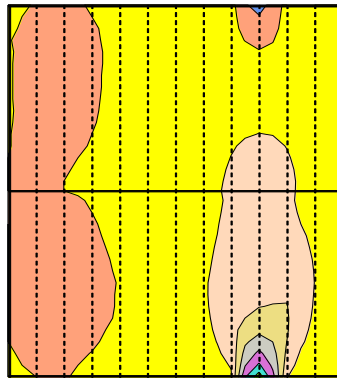


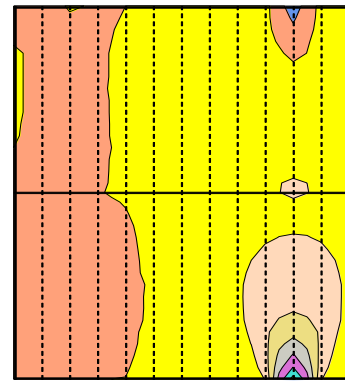
Figure A. 20: Influence coefficient contour for setup 10



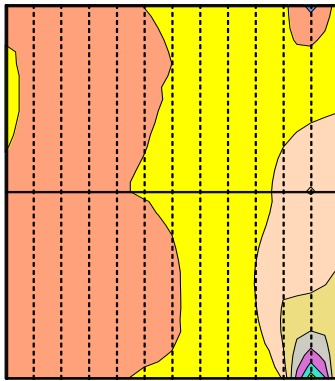
j.



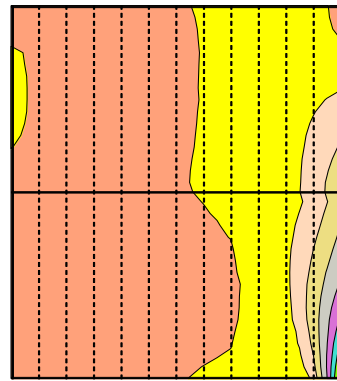
k.



l.



m.



n.

Figure A. 21: Influence coefficient contour for setup 10(contd.)

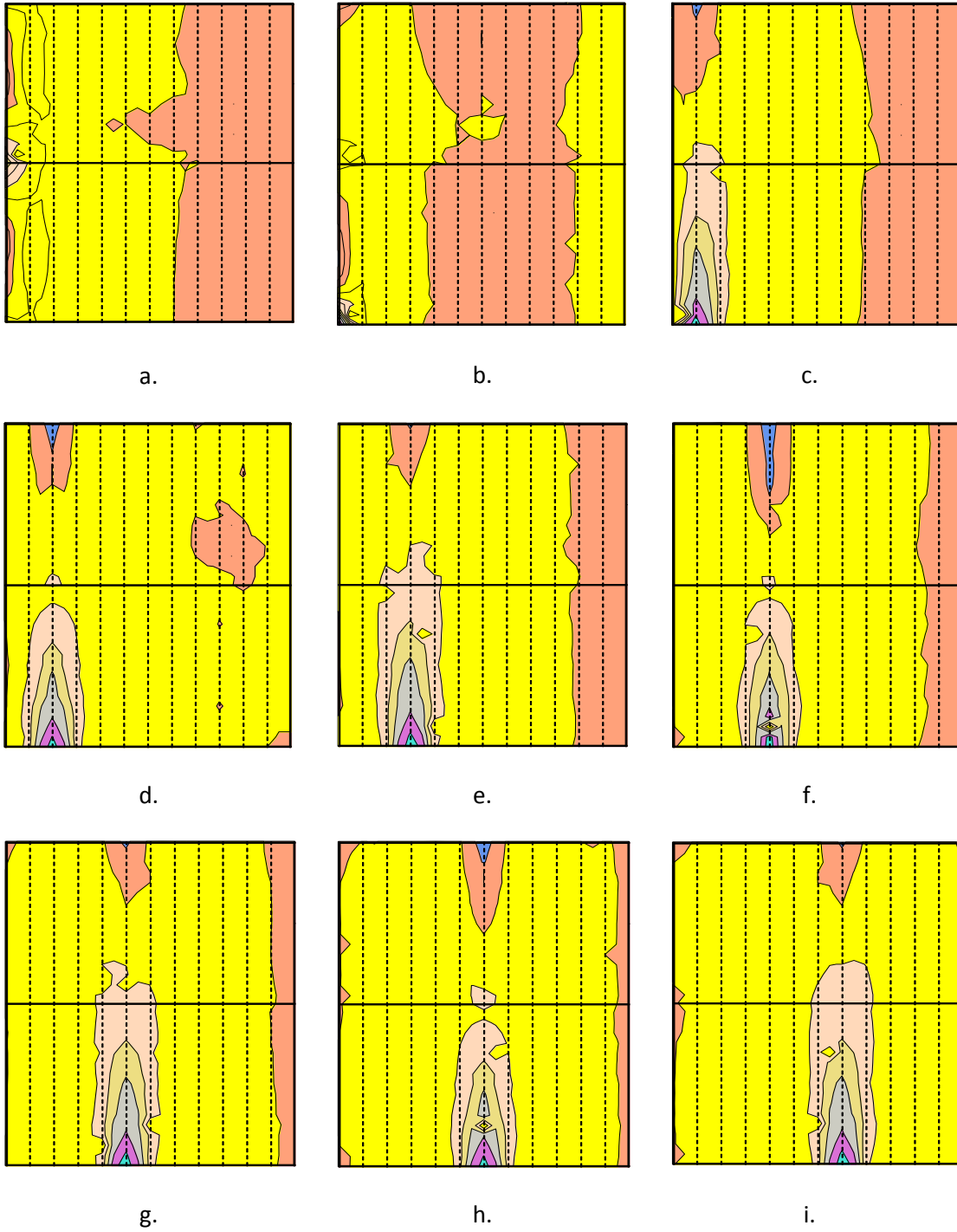


Figure A. 22: Influence coefficient contour for setup 11

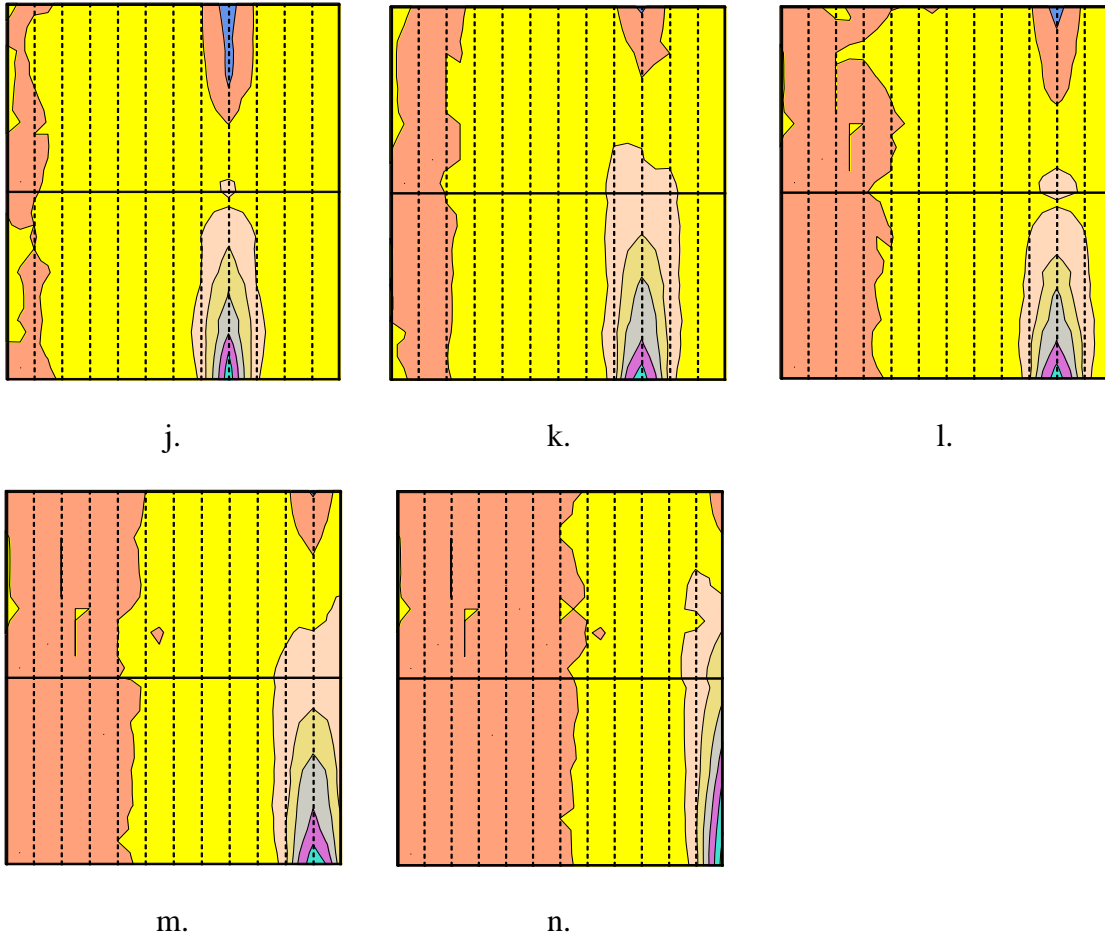


Figure A. 23: Influence coefficient contour for setup 11(contd.)

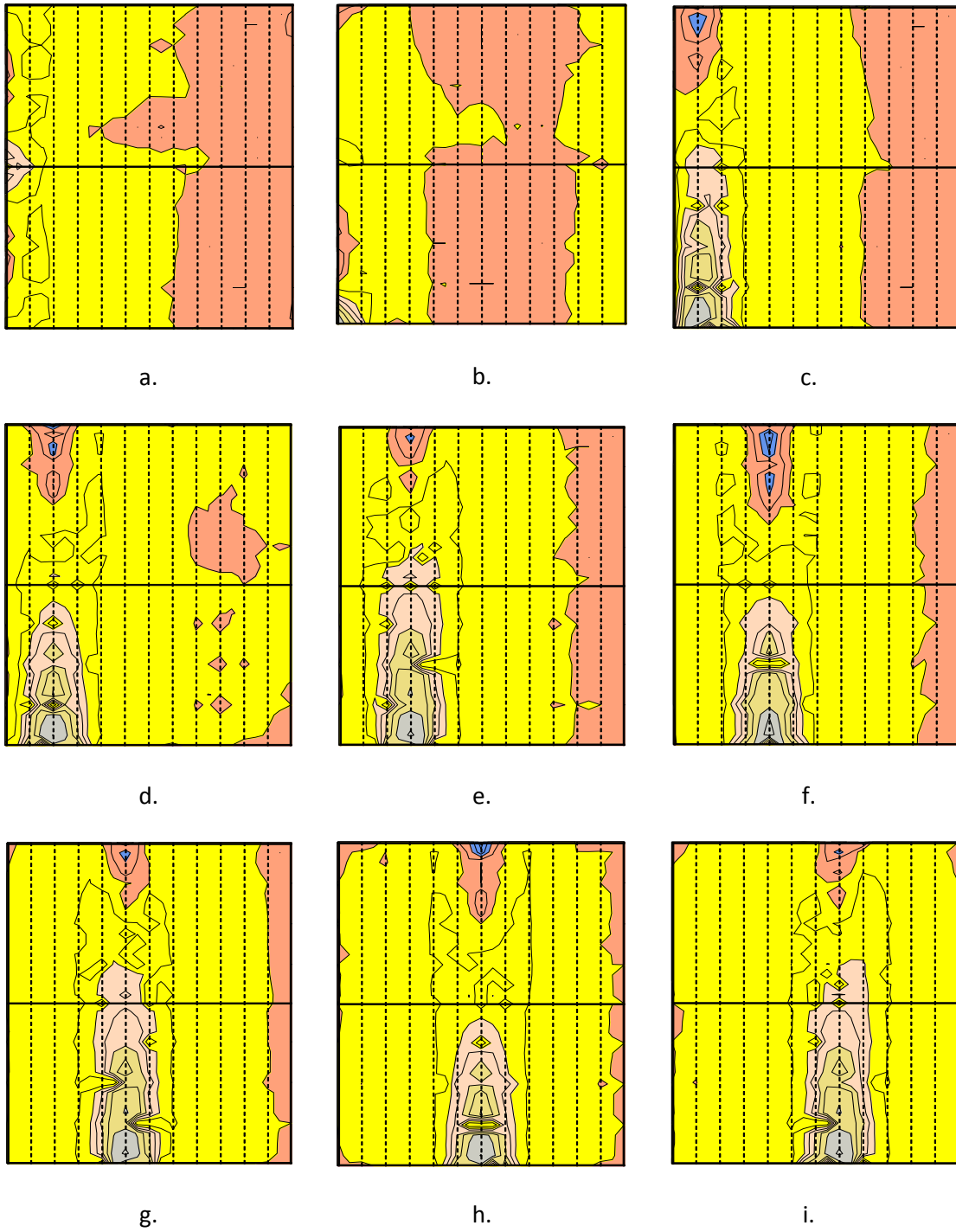
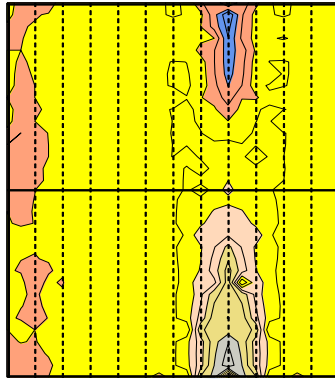
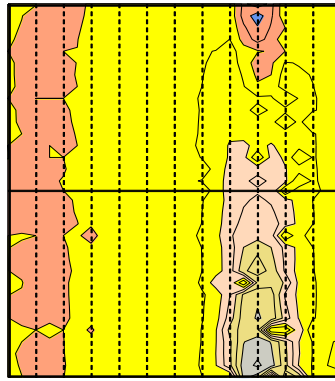


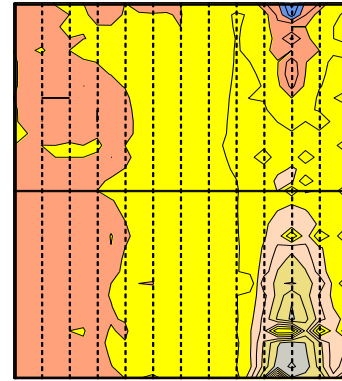
Figure A. 24: Influence coefficient contour for setup 12



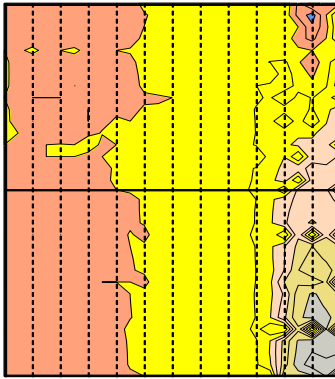
j.



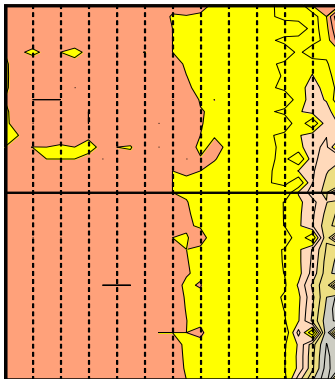
k.



l.



m.



n.

Figure A. 25: Influence coefficient contour for setup 12(contd.)